Czech University of Life Sciences Prague

Faculty of Agrobiology, Food and Natural Resources

Department of Veterinary Sciences (FAFNR)

Master's Thesis

Protein profile of extracellular vesicles isolated from porcine reproductive fluids

Author of the thesis: Bc. Polina Tolkachova

Thesis supervisor: RNDr. Pavla Postlerová, Ph.D.

Consultant: Mgr. Veronika Páleníková, Ph.D.

Declaration

I declare that I have worked on my master's thesis titled "Protein profile of extracellular vesicles isolated from porcine reproductive fluids" by myself and I have used only the sources mentioned at the end of the thesis. As the author of the master's thesis, I declare that the thesis does not break any copyrights.

In Prague on 14.04.2023 _____

Acknowledgement

I would like to express my acknowledgment to Imaging Methods Core Facility at BIOCEV, an institution supported by the MEYS CR (LM2018129 Czech-BioImaging) and Dr. M. Frolíková at the Imaging Core Facility at Institute of Molecular Genetics, CAS, Prague.

This thesis was also supported by the Grant Agency of the Czech Republic GA22-31156S.

I would like to thank RNDr. Pavla Postlerová, Ph.D. and Mgr. Veronika Páleníková, Ph.D., for their guidance, support and encouragement throughout the writing of this thesis. Without their constructive criticism and patience, this work would not have been possible. Finally, I would like to thank my family for their unwavering love, support, and guidance, which have been an invaluable source of strength and comfort during the writing of this thesis.

Protein profile of extracellular vesicles isolated from porcine reproductive fluids

Abstract

Extracellular vesicles (**EVs**) are a promising area of study due to their important role in intercellular communication. These small, membrane-bound particles are present in a wide range of organisms and can be isolated from various body fluids, including semen.

In this study, we used ultracentrifugation and filtration techniques to isolate the EVs fraction from boar seminal plasma. To confirm the presence of vesicles, the isolated fraction was subjected to transmission electron microscopy. Using super-resolution microscopy, we were also able to see interactions between isolated seminal plasma EVs (**sEVs**) and plasma membrane (**PM**) of boar spermatozoon after co-incubation.

With these findings, our next goal was to make a protein profiling of isolated sEVs. For this purpose, we extracted proteins from sEVs under basic and acidic conditions and subjected the samples to mass spectrometry analysis (**MS**). The results of MS for both conditions showed a high abundance of spermadhesin family proteins. However, the presence of tetraspanins and integrins was not confirmed. Additionally, we employed SDS-PAGE and Western blot with four anti-tetraspanin antibodies, which are the typical markers for EVs detection, three anti-spermadhesin antibodies and an antibody against integrin alpha V. We detected strong signals for all spermadhesins and integrin alpha V for both types of protein extraction conditions. However, only a few tetraspanins showed a very weak signal under acidic conditions, while no signal was ever detected under basic conditions during this study.

The potential applications of EVs in reproductive biology are significant, as they have been shown to play important roles in sperm maturation, fertilization, and embryonic development. Our study represents an initial exploration of several methods for the isolation of EVs' fraction from boar seminal plasma and provides valuable insights into the mechanisms behind sEVs' formation in this context. However, further research is needed to elucidate the specific functions of EVs in the boar reproductive system and optimize methods for EVs isolation and characterization.

Keywords: exosomes, tetraspanins, spermadhesins, integrin, ultracentrifugation

Proteinový profil extracelulárních vezikul izolovaných z reprodukčních tekutin prasat

Abstrakt

Extracelulární vezikuly (**EVs**) vzhledem k jejich důležité roli v mezibuněčné komunikaci jsou perspektivní oblasti výzkumu. Tyto malé, na membránu vázané částice jsou přítomny v celé řadě organismů a lze je izolovat z různých tělních tekutin, včetně semenné tekutiny.

V této studii jsme použili ultracentrifugační a filtrační metody k izolaci frakce EVs z kančí semenné plazmy. Za účelem potvrzení přítomnosti vezikul v izolované frakci byla použitá transmisní elektronová mikroskopie. Pomocí superrozlišovací mikroskopie se nám také podařilo zjistit, že izolované z kančí semenné plasmy EVs (**sEVs**) interagují s buněčnou membránou (**PM**) kančí spermie po jejich společné inkubaci.

Na základě těchto zjištění bylo naším dalším cílem vytvořit proteinový profil izolovaných sEVs. Za tímto účelem byla provedena extrakce proteinů ze sEVs za bazických a kyselých podmínek a vzorky byly podrobeny hmotnostně spektrometrické analýze (**MS**). Výsledky MS pro obě podmínky ukázaly vysoký podíl proteinů pocházejících ze spermadhezinové rodiny. Přítomnost tetraspaninů a integrinů však nebyla potvrzena. Dále jsme použili SDS-PAGE a Western blot se čtyřmi protilátkami proti tetraspaninů, což jsou typické markery pro detekci EVs, třemi protilátkami proti spermadhesinů a protilátkou proti integrinu alfa V. U obou typů podmínek proteinové extrakce jsme zjistili silné signály pro všechny spermadheziny a integrin alfa V. Nicméně, pouze několik tetraspaninů však vykazovalo velmi slabý signál za kyselých podmínek, zatímco za zásaditých podmínek nebyl během této studie zjištěn žádný signál.

Bylo prokázáno, že EVs hrají důležitou roli při zrání spermií, oplodnění a embryonálním vývoji, což je významným měřítkem k využití EVs v reprodukční biologii. Naše studie představuje počáteční zkoumání několika metod izolace frakci EVs ze semenné plazmy kanců a poskytuje cenné poznatky o mechanismech, které stojí za tvorbou EVs v tomto kontextu. Nicméně, k objasnění specifických funkcí EVs v reprodukčním systému kanců a k optimalizaci metod izolace a charakterizace EVs je však zapotřebí dalšího výzkumu.

Klíčová slova: exosomy, tetraspaniny, spermadheziny, integrin, ultracentrifugace

Table of content

1 Introduction 8

2 Scientific hypothesis and aims of the thesis 9

3 Literature Review 10

3.1 Extracellular vesicles 10

3.1.1 History 10

3.1.2 Classification and Nomenclature 10

3.1.3 Biogenesis 11

3.1.4 Composition of EVs 13

3.1.5 Lipids 13

3.1.6 Nucleic acids 14

3.1.6.1 RNA 14

3.1.6.2 DNA 15

3.1.7 Proteins 15

3.2 EVs in reproductive fluids 17

3.2.1 Male reproductive fluids 17

3.2.1.1 Epididymal fluid 17

3.2.1.2 Seminal plasma EVs 17

3.2.2 Female reproductive fluids 18

3.2.2.1 Oviductal fluid 18

3.3 Tetraspanins 19

3.3.1 CD9 22

3.3.2 CD81 23

3.3.3 CD151 25

3.3.4 CD63 26

3.4 Methods for EVs' isolation and analysis 26

3.4.1 Ultracentrifugation techniques 27

3.4.2 Ultrafiltration or size-based techniques 28

3.4.3 Immunoaffinity capture-based techniques 28

4 Materials and methods 30

4.1 Materials 30

4.1.1 Raw material 30

4.1.2 Set of antibodies 30

4.1.2.1 Primary antibodies 30

4.1.2.2 Secondary antibodies 30

4.2 Methods 31
4.2.1 Extracellular vesicles isolation from seminal plasma 31
4.2.1.1 Centrifugation 31
4.2.1.2 Differential ultracentrifugation 31
4.2.1.3 Density gradient ultracentrifugation 31
4.2.1.4 Filtration 32
4.2.1.5 Transmission electron microscopy (TEM) 32
4.2.1.6 Protein isolation 32
4.2.1.7 Super-resolution microscopy 33
4.2.1.8 Immunofluorescent Detection of tetraspanins 34
4.2.1.9 Sodium dodecyl sulfate–polyacrylamide gel electrophoresis (SDS PAGE) 34
4.2.1.10 Western blot 35
4.2.1.11 Immunodetection 35

5 Results and Discussion 37
5.1 Results 37
5.1.1 EVs isolation 37
5.1.2 Proteomic study of EVs 38
5.1.3 Interaction of isolated EVs with boar spermatozoon 41
5.1.4 Protein detection of isolated EVs 42
5.1.4.1 Protein profile of sEVs 42
5.1.4.2 Detection of selected proteins in isolated EVs from seminal plasma 43
5.2 Discussion 48

6 Conclusion 52

7 References 53

8 Appendix 64
8.1 Tables 64
8.2 Abbreviations 66

1 Introduction

Extracellular vesicles (**EVs**) are small membranous nanostructures that play an important role in intercellular communication. They carry various types of proteins, nucleic acids, lipids and could transport them from parent cells to recipient cells (Zabrowsky et al. 2015).

A broad distribution of EVs in mammalian organisms suggests that they play a crucial role in various important physiological processes. Their presence has been confirmed in almost all body fluids including blood, saliva, urine, breast milk, bile and cerebrospinal fluid (Colombo et al. 2014). EVs can be identified and studied by their specific markers, such as tetraspanins, integrins, and spermadhesins. One of the most popular markers is considered to be the tetraspanins - a large superfamily of transmembrane protein groups including, for example, CD81, CD63, CD9 (Jankovicova et al. 2020c)

Compared to other mammals, male and female reproductive fluids also contain high levels of heterogeneous vesicle populations. As a model, a boar seminal plasma was chosen to study EVs. Due to the broad functionality of EVs, their involvement in reproductive processes is undeniable. EVs have been shown to regulate different physiological functions related to reproduction, such as fertilization, embryo implantation, and placenta formation. They participate in the regulation of many cellular functions, including cell motility and migration, and they serve as molecular organizers. EVs are also involved in the regulation of immune response and inflammation during pregnancy (Jankovicova et al. 2020c; Yanez-Mo et al. 2015). However, the full range of their physiological roles remains to be elucidated.

The isolation of EVs from biological fluids is still a challenging task due to their small size and heterogeneity. Various techniques have been developed to isolate and characterize EVs, including ultracentrifugation, filtration methods, and immunoaffinity-based methods. Isolation of pure EVs fraction is still a challenge because contamination by other particles is a significant problem. However, the recent studies from Du et al. (2016) and Baranco et al. (2019) succeeded in EVs isolation from boar seminal plasma. They have detected the above-mentioned tetraspanins and a few members of the spermadhesin family proteins. These results could lead us to a better understanding of molecular interaction between EVs and male gametes.

The study of EVs in the context of the reproductive system is an exciting and rapidly evolving field. Although there have been significant advances in our understanding of EVs, there is still much to learn about their roles in reproduction and the underlying mechanisms of function.

2 Scientific hypothesis and aims of the thesis

EVs are small membrane structures that can transfer proteins to spermatozoa during their post-testicular maturation. The content of EVs in the reproductive tract in pigs is not completely known. The aim of the work was to find alternative isolation methods together with the proteomic study of EVs.

Various protocols for EVs' isolation from seminal plasma of boars were used and the protein profile isolated EVs were studied. Proteins were electrophoretically separated and stained, or Western blotted and immunodetected with specific antibodies to selected EVs' proteins, such as tetraspanins, spermadhesins and integrins.

3 Literature Review

3.1 Extracellular vesicles

EVs contain a broad range of membrane nanostructures produced by a cell and released into the extracellular environment. They are essential in cell-cell communication and present in eukaryotic and prokaryotic organisms (Battistelli & Falcieri 2020). In multicellular organisms, EVs are found in all biological fluids, and diverse types of cells can reproduce them (Yanez-Mo et al. 2015).

3.1.1 History

The history of EVs began in the mid-20th century. Chargaff and West (1946) completed studies on the biological significance of the thromboplastic protein of blood, which were carried out by high-speed centrifugation. The experiment revealed a specific subcellular factor that contributed to blood clotting. Later in 1967, electron microscopy identified this subcellular fraction as small vesicles. They were 20 to 50 nm in diameter and 1.020 to 1.025 g/ml in density and were called “platelet dust” (Wolf 1967). Further studies found similar vesicles in different species and tissues, such as fetal calf serum, sheep reticulocytes, human prostatic fluid, and chicken embryonic reticulocytes (Dalton 1975; Johnstone et al. 1987; Ronquist et al. 1978; Johnstone et al. 1991; Grdisa et al. 1993). These vesicles were initially called exosomes. The work of Valadi et al. from 2007 triggered a genuine interest in more detailed studies of EVs when it was suggested that exosomes could transport nucleic acids such as mitochondrial RNA (**mRNA**) and microRNA (**miRNA**). Additionally, according to a later publication, exosomes might have played an essential role in a specific mechanism of removing obsolete transmembrane proteins (Van der Pol et al. 2012). Apart from transporting proteins, lipids, or cell metabolites outside the cell, EVs serve as important genetic information vectors (Colombo et al. 2014). Since then, a new perspective on the possible role of exosomes or other EVs has appeared.

3.1.2 Classification and Nomenclature

A standardized nomenclature for EVs is still under discussion by the scientific community. The reason for different opinions is the lack of a unified classification system (van der Pol et al. 2012) and a standardized method for isolating EVs (Monguio-Tortajada et al. 2019).

Depending on function, composition, size, or origin (tissue culture), many names are suitable for EVs. For example, vesicles derived from the prostate are called prostasomes; from the epididymis - epididymosomes (Sullivan & Saez 2013), from oviductal fluid – oviductosomes (Al-Dossary et al. 2013), etc. Synaptic vesicles gained their name from neurons (Fischer von Mollard et al. 1990); vesicles isolated from tumor cells are called oncosomes (Colombo et al. 2014).

Nowadays, EVs are divided into two main subgroups: exosomes and microvesicles (shedding vesicles/shedding microvesicles/microparticles/**MVs**) (Monguio-Tortajada et al. 2019). However, one can identify apoptotic bodies (**ApoBDs**) as a third subgroup (Battistelli & Falcieri 2020; Yanez-Mo et al. 2015). The key differences between these subgroups are their size, morphology, biogenesis, and intracellular composition.

3.1.3 Biogenesis

The biogenesis of EVs differs depending on the vesicle types. ApoBDs are formed at the late stage of apoptosis from dying cells (Mathivanan et al. 2010), and are later absorbed by tingible body macrophages (Battistelli & Falcieri 2020).

Microvesicles are formed by so-called blebbing (outward protrusion) of the PM. During that process, such enzymes as floppase, scramblase aminophospholipid translocase, gelsolin, and calpain take part. They regulate cell membrane phospholipid asymmetry and subsequent MVs blebbing (Piccin et al. 2007; Mathivan et al. 2010).

On the other hand, exosomes have a more advanced mechanism of biogenesis. It is the so-called endolysosomal pathway (Zhang et al. 2019). Their biogenesis starts from the formation of early endosomes by PM invagination. The early endosomes bud into the surrounding lumina to form intraluminal vesicles (**ILVs**). Inside ILVs, proteins, lipids and nucleic acids are properly concentrated and packed. Early endosomes can conglomerate to form late endosomes or so-called multivesicular bodies (**MVBs**) (Yue et al. 2020; Hessvik & Llorente 2018). The MVBs may fuse with the cell membrane to excrete vesicles or undergo lysosome degradation (Abels & Breakefield 2016).

As shown in **Fig. 1**, there is more than one mechanism for the ILVs and MVBs formation. The endosomal sorting complexes required for transport (**ESCRT**) machinery are the most well-known and well-described. ESCRT consists of about 30 proteins creating 4 major complexes (ESCRT-0, -I, -II, and -III) and associated proteins such as vacuolar protein sorting-associated protein 4A (**VPS4**), tumor susceptibility gene 101 (**Tsg101**), and programmed cell death 6-interacting protein (**ALIX**) (Hanson & Cashikar 2012; Yue et al. 2020). Each of these complexes has a specific function. Thus, for example, ESCRT-0 forms a protein network, recognizes, captures and initiates the sorting of ubiquitinated proteins. The ESCRT-I, in turn, acts as a binding agent providing a linkage between the ESCRT-0 complex and ubiquitinated proteins. It functions as an additional cargo sorting and binding system on endosomes. ESCRT-I also interacts with the ESCRT-II complex. Together, they affect the deformation of the intracellular membrane and its further detachment. ESCRT-III plays a role in exosome formation and release. VPS4, Tsg101, and ALIX proteins work as mediators that support the reaction cascade during the ESCRT mechanism (Yue et al. 2020; Abels & Breakefield 2016; Babst 2011; Zhang et al. 2019).

The ESCRT-independent mechanism can also be an alternative way of exosome formation. During the study of ILVs and exosomes in the mouse oligodendroglial cell line, Trajkovic et al. (2008) noted the high content of cholesterol and sphingolipids such as sphingomyelin (**SM**) and hexosylceramide in exosomes. Later, the author inhibited an enzyme responsible for the production of ceramide (**Cer**) - neutral sphingomyelinase

(**nSMase**). The nSMase inhibition resulted in a marked decrease in exosome release. The author suggested that Cer plays a role in the formation of ILVs, which are later excreted as exosomes. In addition to sphingolipids, phospholipase D (**PLD**) may also participate in exosome biogenesis. PLD metabolizes the transformation of phosphatidylcholine into phosphatidic acid (**PA**). Like Cer, PA also affects endosomal intraluminal budding and provokes the formation of ILVs (Ghossoub et al. 2014).

Stuffers et al. (2009) confirmed that even when all four ESCRT complexes were inhibited, the formation of MVBs and ILVs was not abolished despite minor changes in endocytic compartment morphology. The same author noted the accumulation of CD63 tetraspanin in ILVs in the absence of ESCRT (Stuffers et al. 2009). Later, van Niel et al. (2011) confirmed the importance of CD63 involvement in the ESCRT-independent process of premelanosome protein (**PMEL**) luminal domain sorting in melanosomes. However, in addition to CD63, other members of the tetraspanin family may also be involved in exosome biogenesis. Chairoungdua et al. (2010) demonstrated β-catenin exosome release enhancement via the Cer-dependent exosomal pathway by overexpression of CD81 and CD9 tetraspanins. Later, Perez-Hernandez et al. (2013), citing their data, pointed out that CD81 knockout disrupts the selective repertoire of CD81-interacting molecules in exosomes. Presumably, the exosome biogenesis mechanism depends on the cell's origin, type, and compartment composition.

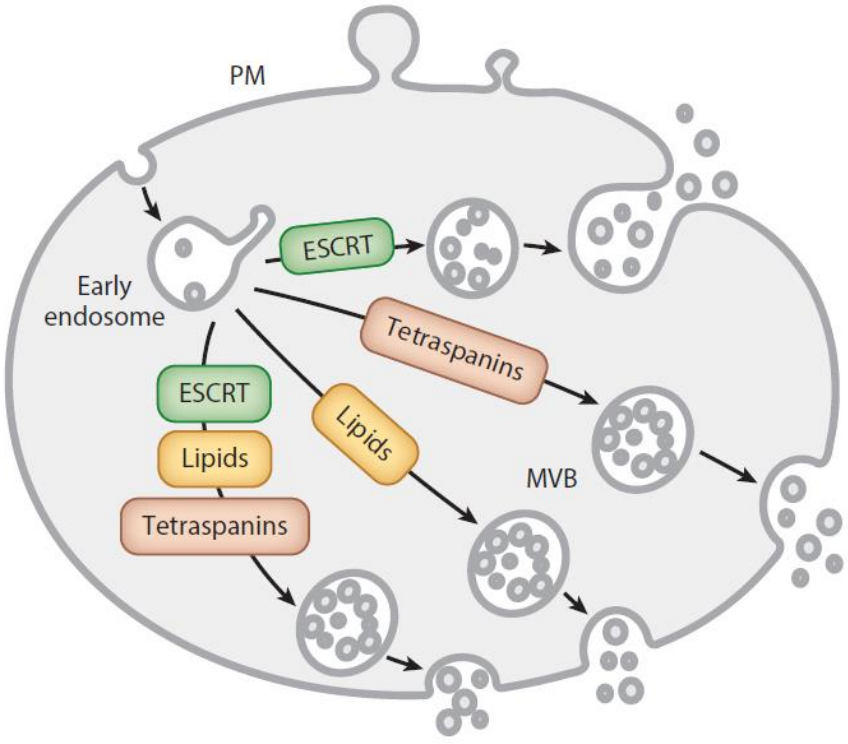

Figure 1: Schematic representation of main exosome biogenesis mechanisms by *Colombo et. al (2014)*. ESCRT – endosomal sorting complexes required for transport, which is the most well-described mechanism of exosome biogenesis. Tetraspanins and Lipids are other biogenesis mechanisms that can affect the formation of exosomes either independently or in combination with the ESCRT. Abbreviation: PM – plasma membrane; MVB – multivesicular bodies.

3.1.4 Composition of EVs

The content of EVs could include numerous classes of proteins, lipids and different forms of nucleic acids. The overall content of EVs is shown in **Fig. 2**. Their composition depends on the specific tissue culture from which they originated (Zabrowski et al. 2015). There are currently several sources dedicated to the study of EVs. They include databases with the EV composition derived from multiple organisms. The most popular are ExoCarta (http://www.exocarta.org/), Vesiclepedia (http://microvesicles.org/) and EVpedia (http://evpedia.info).

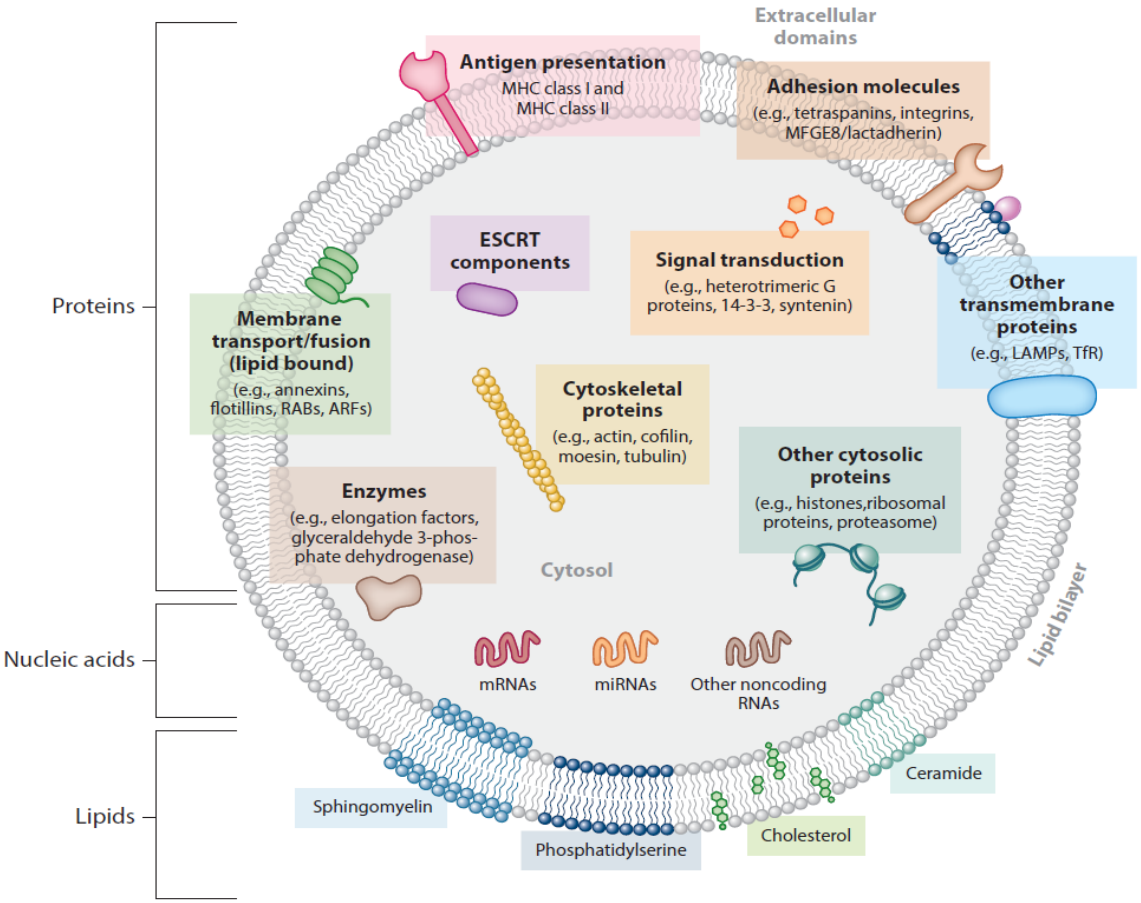

Figure 2: The schematic representation of basic EV protein, nucleic acid and lipid content. However, it should be noted, that each of the listed components may be present in some subtypes of EVs, but not in others. The specific number of vesicle content depends on their origin and main functions (*Colombo et al. 2014*).

3.1.5 Lipids

Like a cell membrane, the EVs membrane consists of a lipid bilayer. However, the composition of the EVs' bilayer is specific and differs from the parent cells. Many studies have shown that the EVs' membrane is rich in cholesterol (**Chol**), SM, phosphatidylserine, unsaturated lipids (**UL**), gangliosides (Laulagnier et al. 2004; Llorente et al. 2013; Trajkovic et al. 2008; Wubbolts et al. 2003), Cer (Kalra et al. 2016) and glycosphingolipids (Yanez-

Mo et al. 2015). During EVs' studies using Laurdan fluorescence spectroscopy, it was proved that the increased content of SM, Chol, and DL provides structural rigidity to the EVs membrane. It makes the membrane more stable compared to the parent cell. The pH level could also affect the rigidity of the EV membrane. During experiments held by Laulagnier et al. (2004), a membrane of EVs derived from basophils (RBL-2H3) became less rigid when treated with an acidic solution. In another study by Parolini et al. (2009), different pH conditions were used as a modifier of exosome traffic. The results showed that high acidity levels in the tumor microenvironment increased cancer cells' release and uptake of EVs. Thus, a low pH level reduces the EV membrane rigidity by increasing its fluidity and making it more similar to the cell PM (Zabrowsky et al. 2015).

The next difference in the EV membrane from the parent cell membrane is higher transverse diffusion (flip-flop rate) and lower lateral membrane diffusion (Carroll-Portillo et al. 2012). The combination of the above-mentioned chemical and biophysical properties contributes to the EV membrane resistance to degradation in the extracellular environment. It allows EV to transport various biomolecules to the other cells (Huang et al. 2013; Ridder et al. 2014).

3.1.6 Nucleic acids

3.1.6.1 RNA

The RNAs found in the EVs are called EV-RNAs. The identification and further study of this type of nucleic acid in the EVs are carried out using the high-throughput RNASeq method, microarray analysis, and transcript-specific RT-qPCR analysis (Kim et al. 2017). Nowadays, it is currently known that the average size of the EV-RNA nucleotide chain is approximately <700 nucleotides. Many different types of RNA have been found in the EVs. They are long non-coding RNA (**lncRNA**), mRNA, miRNA, intact mRNA, ribosomal RNA (**rRNA**), and piwi-interacting RNA (**piRNA**) (Yanez-Mo et al. 2015). Also, there can be found small nucleolar RNA (**snoRNA**), circular RNA (**circRNA**), small nuclear RNA (**snRNA**), and transfer RNA (**tRNA**) (Kim et al. 2017). It has also been noted that 18S and 28S rRNA are present in EVs either in small amounts or absent at all (Crescitelli et al. 2013; Nolte-'t Hoen et al. 2012). However, the size and types of RNA can vary depending on the type of cell that produces EVs. Also, the determination of EV-RNAs nucleotide length can be strongly affected by sample purity and EVs isolation technique (Zabrowsky et al. 2015). For example, samples with isolated EVs can show false positive results for the presence of extraneous nucleic acids. Ribonuclease (**RNase**) and deoxyribonuclease (**DNase**) can be used to eliminate unwanted nucleic acids and avoid contamination outside the EVs. There is no risk of damaging EV-RNAs or EV-DNAs during the decontamination procedure because the rigid membrane of EVs protects the luminal nucleic acids from external damage (Miranda et al. 2010).

Despite a vast number of common transcripts, some EV-RNA profiles may not coincide with RNA profiles of parent cell (Zabrowsky et al. 2015). The inclusion and exclusion regulation pathways of specific transcripts in EV-RNA remain unknown. However, it has been suggested that this regulation process may be related to the activity of

RNA-binding protein (**RBP**) complexes and ribonucleoprotein particle (**RNP**) granules (Kim et al. 2017).

The primary function of EV-RNAs is to transfer genetic information and change the gene expression in recipient cells. With a better understanding of these processes, EVs could become important vectors for delivering various molecules to target tissue for therapeutic purposes (Colombo et al. 2014).

3.1.6.2 DNA

Similarly, as with RNA, DNA found in EVs is called EV-DNA. However, unlike EV-RNA, EV-DNA is not that commonly studied. Nowadays, a few different DNA types, such as single-stranded DNA (**ssDNA**), double-stranded DNA (**dsDNA**), mitochondrial DNA (**mtDNA** / **mDNA**), and viral DNA, were found in EVs (Elzanowska et al. 2020).

Interestingly, DNA can be found not only in the EV lumen but also attached to the outer layer of EVs membrane. The DNA inside the EV is more protected from extracellular environmental exposures. It provides a significant advantage primarily for viral DNA and tumor-derived vesicles, which can thus avoid recognition by the immune system (Lazaro-Ibanez et al. 2014). The size of the DNA inside the EVs varies from 100 base pairs to 2.5 kilobase pairs. The outer DNA is larger (>2.5 kb) than the luminal DNA (Thakur et al. 2014). EV-DNAs can be used as a translational biomarkers to identify mutations in parental tumor cells. EV-DNAs biomarkers can contribute a lot as a method of cancer disease diagnosis and prognosis (Yanez-Mo et al. 2015).

3.1.7 Proteins

Proteins are probably one of the main and most numerous types of EVs cargo. Therefore, the protein composition of EVs is very rich and diverse and depends on the type of cell that produces these vesicles, the function that the vesicle should perform, and the type of the vesicle itself (Zabrowsky et al. 2015). However, there is still a certain common set of proteins characteristic of most vesicles regardless of their cellular origin. For example, because of their endosomal origin, the ESCRT, ALIX, and Tsg101 proteins, which are involved in MVB formation, can be detected in exosomes. It is also characteristic for them to have proteins responsible for cell fusion, signalling, adhesion and transport, and exosome release. These proteins include integrins, annexins, flotillin-1, Rab GTPases, tetraspanins (CD53, CD63, CD86, CD9, etc.), transmembrane glycoprotein markers for lysosome such as lysosomal-associated membrane proteins (LAMP1 and LAMP2). Also, exosomes contain proteins responsible for structural integrity and degradation, such as ubiquitin and heat shock proteins (HSP70, HSP90); and protective function (class I and II of major histocompatibility complex) (Kalra et al. 2016; Thery et al. 2001; Palmisano et al. 2012; Raposo & Stoorvogel 2013).

MVs have a different set of proteins compared to exosomes because they originated from the PM. For example, they tend to contain glycoprotein Ib, arrestin-containing protein 1 (Heijnen et al. 1999). However, they also have proteins shared with exosomes, such as TSG101, which interacts with other proteins (Nabhan et al. 2012). ApoBDs carry their

specific proteome, most often represented by the DNA-binding histones such as H3, H2B, H2A, H4 (Thery et al. 2001).

3.2 EVs in reproductive fluids

3.2.1 Male reproductive fluids

3.2.1.1 Epididymal fluid

During transit through the epididymis and other accessory sex organs, testicular spermatozoa must undergo morphological and functional changes to become fully fertile. Most possible spermatozoa enrichment could be provided by different types of vesicles, such as epididymosomes and prostasomes. Numerous studies have demonstrated the presence of EVs released in an apocrine manner by principal cells into the lumen of the epididymal duct in humans (Yeung et al. 1997; Thimon et al. 2008), bulls (Girouard et al. 2011), mice (Rejraji et al. 2002), Chinese hamsters (Yanagimachi et al. 1985), rats (Fornes & De Rosas 1991) and rams (Gatti et al. 2002). Depending on their region of origin (cauda, corpus or caput), the epididymosome population is highly heterogeneous and carries different types of proteins. Epididymosomes play a protective role for spermatozoa during their epididymal transit and help them to become fertilization-competent (Gervasi et al. 2017; Sullivan & Saez 2013; Girouard et al. 2011). For example, the isoform of the plasma membrane calcium ATPase (**PMCA4**) protein is also secreted in the epididymal luminal fluid and is carried, presumably by vesicles, to the spermatozoa and contributes to their hyperactivated motility (Al-Dossary et al. 2013). Other molecules that have been detected in epididymosomes include chaperones, structural proteins, enzymes, signal transductors and adhesion molecules (Girouard et al. 2011).

3.2.1.2 Seminal plasma EVs

Ejaculated semen involves the mix of spermatozoa with seminal plasma (**SP**) components, which are derived from the accessory sex glands. Despite the differences between the species, SP contains common components such as ions (K^+, Na^+, Zn^+, $Ca2^+$, $Mg2^+$), energy substrates (fructose, sorbitol, glycerylphosphocholine), organic compounds (citric acid, aa, peptides, proteins, lipid, hormones, cytokines), nitrogenous components (Juyena & Stelletta 2013), etc. A lot of these components are carried by different types of seminal EVs (**sEVs**).

Several studies confirm the presence of a heterogeneity population of EVs in humans (Ronquist et al. 1978), bulls (Alves et al. 2021), stallions (Arienti et al. 1998; Twenter et al. 2020), ram (Leahy et al. 2020) and boar SP (Du et al. 2016; Barranco et al. 2019; Xu et al. 2020). Despite this, the exact physiologic role of EVs in SP remains poorly evaluated and far from being fully understood (Roca et al. 2022). However, Du et al. (2016) reported, that boar SP vesicles could transfer and bind proteins to sperm and maintain a protecting role, such as antioxidation and inhibition of premature sperm capacitation. Another study by Barranco et al. (2019) succeeded in the isolation of two different sEVs subtypes (exosomes and MVs). They also confirmed the presence of the tetraspanins CD9, CD81, CD63 in the boar SP, with varying levels of expression. It has been suggested that these tetraspanins can serve as biomarkers to confirm vesicle isolation (Barranco et al. 2019).

3.2.2 Female reproductive fluids

3.2.2.1 Oviductal fluid

The presence of EVs in the female reproductive fluids plays a major role in the process of oocyte maturation, successful fertilization and even embryo-maternal communication (Jankovicova et al. 2020c; Alminana et al. 2017). One of these vesicle types is called oviductosomes (**OVs**), which, based on their name, are found in the oviductal fluid (**OF**). OVs have been successfully isolated in several animal species such as mice (Al-Dossary et al. 2013; Fereshteh et al.2018), cattle (Alminana et al. 2017; Lopera-Vasquez et al. 2016), canines (Lange-Consiglio et al. 2017), humans (Bathala et al. 2018), chickens (Huang et al. 2017) and even turtles (Waqas et al. 2017). Bathala et al. (2018) have reported the presence of OVs in mice and women OF. They confirm, that vesicles are arising via the apocrine pathway, and they are responsible for carrying fertility-modulating proteins, such as PMCA4 and PMCA1. The most likely function of these vesicles is cell-cell communication, which mediates the transfer of PMCA4 and PMCA1 proteins from OF to spermatozoa during their capacitation (Bathala et al. 2018; Al-Dossary et al. 2013). Apart from protein delivery function, OVs are also responsible for transferring nucleic acids from OF to spermatozoa. Fereshteh et al. (2018) proved the presence of 272 types of miRNAs in mouse OVs. They suggest that some of the miRNAs are enriched with transcription factors and regulators, protein kinases, and genes that are involved in the first cleavage of the zygote during embryonic development (Fereshteh et al. 2018).

3.3 Tetraspanins

Tetraspanins belong to the transmembrane 4 superfamily (**TM4SF**) proteins. These relatively small integral proteins (about 200-350 amino acids (**aa**)) have been found and intensively studied in numerous species like fungi, plants, amoebae, flatworms, insects, and fish, as well as in mammals. For example, the human genome encodes 33 tetraspanin family members. Tetraspanins play a fundamental role in the organization of normal and pathological processes in the organism. Depending on the cell type and the interacting protein composition, they may participate in various cellular processes. For instance, tetraspanins assist in endocytosis and exosome formation, cell migration, adhesion, penetration, and mediating signalling cascades. Tetraspanins are involved in generating an immune response. They promote the release of viruses and other pathogens and participate in tumor development and metastasis. (Lang & Hochheimer 2020; Reppert & Lang 2022).

The names of tetraspanins do not have a precise nomenclature. One can, for example, classify tetraspanins based on a "cluster of differentiation" (**CD**), such as CD9, CD53, CD63, CD81, and CD151. Another nomenclature refers to tetraspanins by their type of tissue origin. For instance, tetraspanins isolated from the urothelium are called uroplakins. As an example of more systematic nomenclature can serve the human Tspan1-33 or the basidiomycete *Cryptococcus neoformans* Tsp2-type protein. Some proteins may have more poetic names, such as Sunglasses or Late Bloomer found in Drosophila melanogaster. However, despite all the diversity, the names of tetraspanins do not reflect their functions or structural features (Reppert & Lang 2022).

Presently, the most structurally studied tetraspanins are human CD81 and CD9. They serve as the primary model for understanding the chemical-physical properties, their functions, and the principle of interaction with each other and other molecules (Huang et al. 2005; Lang & Hochheimer 2020; Yang et al. 2020).

Based on a structure of a CD81, tetraspanin protein can be structurally divided into three regions - cytoplasmic, transmembrane, and extracellular domains. N- and C- protein tails point into the cytosol from the inner part of a PM, forming the intracellular domain. This region is important for the determination of protein functional specificity. For example, different C-terminus amino acid motifs can mediate the proper intracellular localization. Also, tetraspanins can be sorted out based on a slight motif's differences or provide a link for intracellular interacting proteins.

Tetraspanin consists of four transmembrane microdomains (**TMs** 1-4) – specialized structures in PM. These microdomains protrude from the outer side of PM in four places. A short aa sequence (presumably 4 aa long) connects TM2 and TM3 microdomains from the inner side of PM (Yanez-Mo et al. 2009) (see **Fig. 3**).

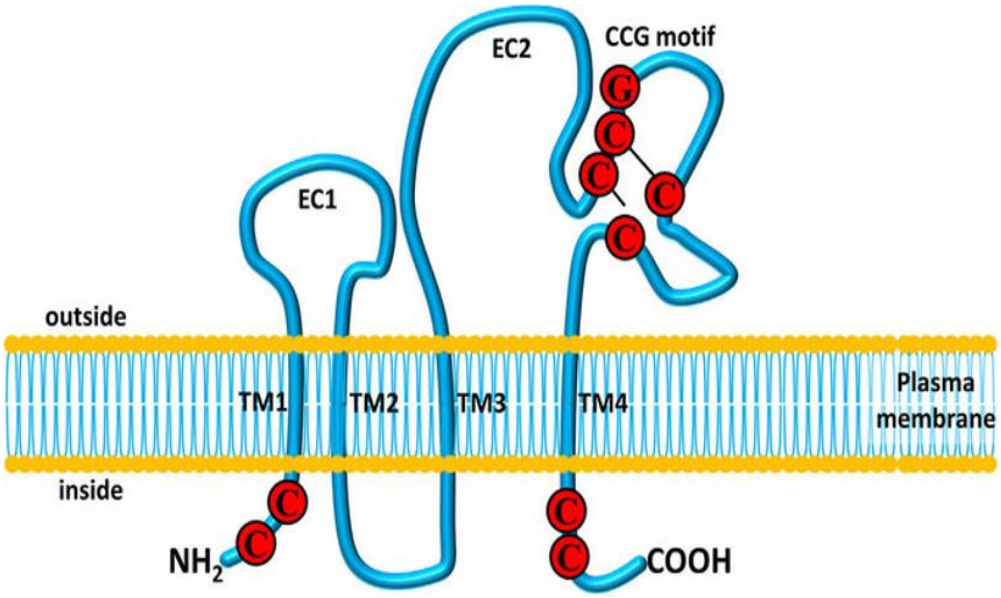

Figure 3: Schematic structure of tetraspanin by *Zou et al. (2018)*. EC1– small extracellular loop; EC2 – large extracellular loop; TM1-4 – transmembrane microdomains.

Apart from the four TMs, tetraspanin consists of two unequally-sized extracellular regions. One of them is a small extracellular loop (**EC1** / SED / SEL) containing 20 – 28 aa, and the second is a large extracellular loop (**EC2** / LED / LEL) containing 76 - 131 aa (Boucheix & Rubinstein 2001) (see **Fig. 3**). In some tetraspanin isoforms, a small extracellular loop is quite diverse and sometimes can be glycosylated, although the exact function of the post-translational modification is still poorly understood. (Andreu & Yanez-Mo 2014; Reppert & Lang 2022). However, the study of Yang et al. (2020) suggests that EC1 interacts with a large extracellular loop to maintain the open tetraspanin conformation (see **Fig. 4**), which promotes tetraspanin-partner interactions. Compared to the EC1 loop, EC2 is a more well-studied region. Its structure has a "mushroom-like" shape and is considered to act as a binding region. EC2 consists of a constant region with three conserved helices (A, B, and E) and a variable region with two helices (C and D). C and D helices form the most distant region from a PM and are responsible for protein-protein interactions (Andreu & Yanez-Mo 2014; Yang et al. 2020). A distinctive feature of EC2 is the presence of a conserved aa motif CCG-motif (Cys-Cys-Gly) and several conserved cysteine residues that form disulfide bonds. Also, tetraspanin molecules have different structural features depending on their functions in specific cellular processes. In tetraspanin structure, several specific motives and aa sequences can often occur, such as the Pro-Xaa-Xaa-Cys (PXXC) motif, the YXXØ motif (Tyr-Xaa-Xaa-Ø), the Gly-Tyr-Glu-Val-Met (GYEVM) sequence, etc. (Andreu & Yanez-Mo 2014; Termini & Gillette 2017; Berdichevski & Odintsova 2007).

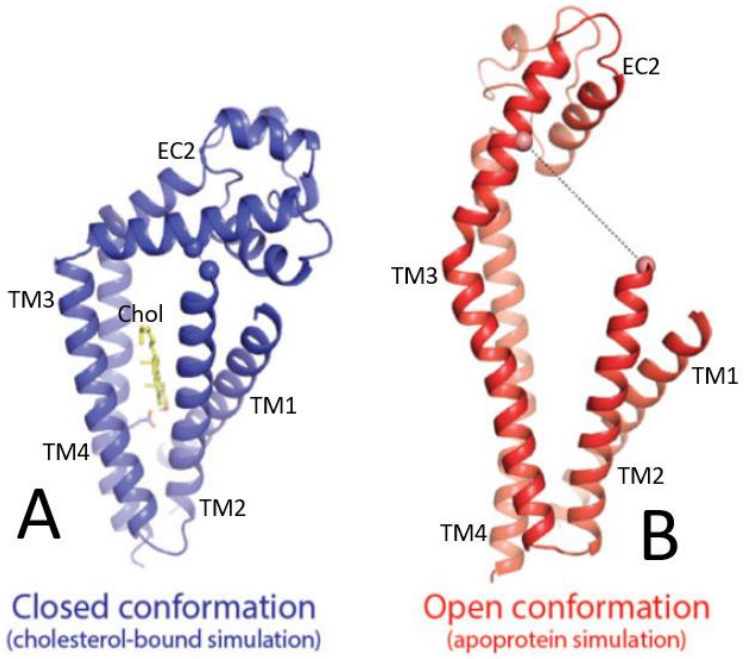

Figure 4: Closed (**A**) and open (**B**) conformations are performed in molecular dynamics simulations. After cholesterol removal, tetraspanin molecule is transitioned to an open conformation, and EC2 is disengaged from TM1 and TM2 (*Zimmerman et al. 2016*).

Like many other proteins, tetraspanins undergo various post-translational modifications. One of these is the N-terminus ubiquitination, which plays a vital role in the regulatory mechanism of selective cell signaling attenuation (Termini & Gillette 2017). The second significant modification is palmitoylation. Palmitate attaches to intracellular cysteine residues (Charrin et al. 2014), promoting and regulating the formation of tetraspanin-tetraspanin interactions and tetraspanin-enriched microdomains (**TEMs**). Also referred to as the «tetraspanin web» (Termini & Gillette 2017; Deventer et al. 2017).

The tetraspanin web is a hierarchical network of interactions that binds tetraspanins to a certain number of proteins and plays a major role in cell-cell interactions and cell-fusion events. The interactions of tetraspanin molecules with their partners are divided into three levels. The primary (first-level) interaction is a covalent bond resistant to degradation by strong detergents, which can be either homophilic (tetraspanin-tetraspanin) or heterophilic (tetraspanin-partner). The secondary (second-level) interaction binds homophilic and heterophilic primary complexes together; this interaction is more vulnerable to destruction and can withstand only weak detergents. Also, secondary complexes are sensitive to disruption of palmitoylation since this modification affects the formation of bonds between the complexes. The tertiary (third-level) interaction structural complex is very fragile. It is resistant only to weak detergents (such as 1% Brij-99 and CHAPS107). These detergents could also work as detectors of these complexes (van Deventer et al. 2017; Hemler 2005; Claas et al. 2001).

The major tetraspanin partner proteins are integrins (α3β1, α6β1, α6β4, LFA-1, etc.), immunoglobulin superfamily proteins (EWI-2, EWI-F, ICAM-1, VCAM-1, etc.), metalloproteinases (ADAM10, ADAM17, ADAM3 etc.) and activated protein kinase C (**PKC**) isoforms. Each of these interactions performs a whole cascade of different physiological processes. These include the interaction of tetraspanins with EVs, which play an important role in mammalian fertilization. The best-known tetraspanins that contribute to both the female and male reproductive systems and also interact with EVs, are CD9, CD151, CD81, and CD63 (Rubinstein 2011; Andreu & Yanez-Mo 2014; Hemler 2005; Jankovicova et al. 2020b).

3.3.1 CD9

CD9 is a low tissue specificity protein with a molecular mass of 24-27 kDa. The function of CD9 is the best studied among other tetraspanins in the reproduction field. It has been found in the gametes of such mammals as mice (*Mus musculus*), rats (*Rattus norvegicus*), cattle (*Bos taurus*), humans (*Homo sapiens*), and pigs (*Sus scrofa*) (Kaewmala et al. 2011; Miyado et al. 2000; Jankovicova et al. 2015; Zhou et al. 2009).

The Kanatsu-Shinohara et al. (2004) study confirmed the expression of this protein in mouse and rat male spermatogonial stem cells. In the Kaewmala et al. (2011) study, CD9 mRNA transcripts were found in boar testes, epididymis, accessory glands, and other parts of the reproductive tract, including Leydig and Sertoli cells. CD9 protein was also found on the bovine sperm PM (Cupperova et al. 2014; Antalikova et al. 2015). CD9 protein is present in many reproductive tissues and different developmental stages of male germ cells. That observation suggests that CD9 plays an essential role in spermatogenesis and the further maturation of spermatozoa in the female reproductive tract. Another study (Antalikova et al. 2015) suggested that CD9 can support fertilization by forming multimolecular complexes on the bovine sperm PM. Also, by identifying the common CD9 surface antigen on spermatogonial stem cells, methods for restoring impaired men's spermatogenesis function after chemotherapy or radiotherapy can be developed (Kaewmala et al. 2011; Kanatsu-Shinohara et al. 2004).

The important presence of CD9 on the oocyte during fertilization has been confirmed in several experiments using CD9 knockout (CD9-/-) females and male mice. Male CD9-/- mated with wild-type (CD9+/+) females were fertile, and their spermatozoa had no problems penetrating the oocytes. However, problems occurred in the CD9-/- females. They were born healthy, grew normally, and even had standard indicators of healthy ovulation. Nevertheless, after in vivo copulation, their litter size was less than 2% of the wild type. Infertility was also frequently observed (Kaji et al. 2000, Miyado et al. 2000). Using in vitro fertilization (**IVF**), Miyado et al. (2000) determined that spermatozoa could not fuse with the PM of the CD9-/- oocyte after penetration of zona pellucida (**ZP**) and accumulated in its perivitelline space (PVS). There was also an experiment with intracytoplasmic sperm injection (**ICSI**) of wild-type spermatozoa into the cytoplasm of CD9-/- oocytes, which resulted in successful fertilization and further embryo development. As a conclusion of their experiments, the authors suggested that CD9 deficiency on the oocyte membrane affects the process of

oocyte-sperm fusion but not the subsequent processes of embryo development. In more recent studies, Miyado et al. (2008) studied the effect of CD9 on sperm-egg interaction in mice and found that gamete fusion depends on the release of CD9-positive vesicles from the oocyte into its PVS.

Because CD9 is expressed in different cells, it can serve as a marker for exosome identification. In addition to CD9, the most common tetraspanins associated with exosomes are CD63, CD81, and CD82 (Escola et al. 1998; Mathivanan et al. 2010). CD9-positive vesicles were found on oocytes and embryos of humans (Vyas et al. 2019), mice (Miyado et al. 2008), pigs (Li et al. 2004), and cows (Mellisho et al. 2017). The secretion of CD9-positive vesicles was observed on the oolema surface and, as previously mentioned by Miyado et al. (2008), in the oocyte's PVS. It is also interesting that EVs have not been detected in the ZP of mature metaphase II oocytes. However, immediately after fertilization and zygote formation, intense secretion of EVs can be observed throughout the ZP (Vyas et al. 2019). Also, Vyas et al. (2019) found solid CD9 signalling in EVs in human preimplantation embryo development, including 1-cell zygotes, cleavage embryos (2-cell, 4-cell, and 8–10-cell), morulae, and blastocysts, including a compromised blastocyst which only contained the trophectoderm layer and no inner cell mass. Ng et al. (2013) also found secretion of CD9 and CD63 exosomes containing specific miRNAs on the apical surfaces of endometrial epithelial cells in the woman's uterus. It was suggested that specific miRNAs might enhance the invasive potential of trophoblast cells and be important for embryo implantation. It has also been suggested that EVs secreted by both trophectoderm cells and endometrium may participate in bidirectional intercellular communication between mother and embryo and potentially modulate the maternal immune system (Bidarimath et al. 2017; Kshirsagar et al. 2012; Vyas et al. 2019).

Caballero et al. (2013) confirmed the presence of CD9-positive microvesicles in bovine epididymal fluid, which, unlike epididymosomes, were enriched with different proteins. Also, CD9 protein was detected in epididymal epithelial cells in all epididymis regions, with higher levels of expression in the apical margins of the cauda region. It was suggested that CD9-positive microvesicles could play a role in transporting GliPr1L1 and P25b proteins - involved in sperm-ZP interaction – to the acrosomal region of spermatozoa during their epididymal transit. In addition to this function, enriched MVs' microdomains with this tetraspanin could potentially protect spermatozoa from oxidative stress and participate in cell-cell communication (Caballero et al. 2013; Frenette & Sullivan 2001).

3.3.2 CD81

The next tetraspanin that is important in successful mammalian fertilization is CD81. The structure of this protein, with a molecular weight of about 26 kDa (Boucheix & Rubinstein 2001), is a classic and well-studied model of the tetraspanin family. A common molecular partner of CD81 is the previously described CD9, which has 45% aa sequence homology with CD81 in all four transmembrane regions (Jankovicova et al. 2016; Boucheix & Rubinstein 2001). The co-localization of these tetraspanins has been found on the head of human spermatozoa. However, when these two tetraspanins interact on gametes, they

perform slightly different functions. By binding and releasing cholesterol, CD81 is able to regulate PM bending of the sperm head, while CD9 stabilizes the tetraspanin network and facilitates the role of tetraspanin trans-interactions with other proteins. As a result, the CD81/CD9 interaction plays an important role in the process of gamete fusion (Frolikova et al. 2018).

The surface of PM of murine oocytes was the first mammalian gamete in which CD81 tetraspanin expression was confirmed (Takahashi et al. 2001). However, the conclusions about the exact localization of this protein vary among different authors. Ziyyat et al. (2006) confirmed the presence of positive tetraspanin CD81, CD9, and CD151 signals in PM of human oocytes. Later, during the staining of mouse oocytes, Tanigawa et al. (2008) noted that CD81 was more expressed in granulosa and cumulus cells than on the oocyte PM. Later Ohnami et al. (2012), also studying mouse oocytes, confirmed that the bulk of CD81 production occurs in cumulus cells. They also indicated that later this protein is localized on the ZP. The results of Jankovicova et al. (2016) were slightly different. By studying bovine oocytes, the author confirmed the expression of CD81 in cumulus cells and PM of germinal vesicle (**GV**), MI, and MII oocytes. However, on the ZP in several oocytes' developmental phases, including those matured to MII in vitro, were not detected any positive CD81 signal. CD81 was also detected on PM in the form of organized clusters on the inner margin of ZP and PVS of porcine oocytes (Jankovicova et al. 2019).

Compared to oocytes, studies about the role of CD81 and its localization on mammalian spermatozoa are relatively recent. Jankovicova et al. (2016) examined and confirmed the expression of this protein in the apical region of the head of epididymal and ejaculated bull spermatozoa, as well as on the PM covering the apical acrosome in mouse spermatozoa. A few years later, Frolikova et al. (2018) confirmed the presence of CD9 and CD81 in the apical acrosomal area in human spermatozoa. In this research, the presence of CD81 on mouse epididymal spermatozoa was also proved (Frolikova et al. 2018), and the conclusion of its localization was similar to the previous author (Jankovicova et al. 2016).

It is also worth mentioning the change in the location of CD81 on the spermatozoa during the reactions that occur in the female genital tract after copulation. For example, acrosome reaction (**AR**) results in the relocalization of CD81 to the equatorial segment in the mouse model. On the other hand, CD81 disappears from the apical acrosomal area but remains detectable in the post-acrosomal area of the sperm head in humans. In bovine spermatozoa, this protein completely disappears after AR. In contrast to AR, the capacitation result did not show any changes to CD81 location in all three species (Jankovicova et al. 2016; Frolikova et al. 2018). Jankovicova et al. (2016) also suggested that the presence of CD81 on spermatozoa can serve as a distinctive marker of acrosome intactness.

A 40% fertility reduction was observed due to experiments with CD81 gene knockout in female mice. While deletion of CD9 and CD81 led to sterility and aggregation of some spermatozoa in the PVS. This only confirms the importance of the participation of these two tetraspanins in gamete fusion (Rubinstein et al. 2006). However, in experiments with CD81 and CD9/CD81 knockout, in male mice, the absence of these tetraspanins did not affect their sperm ability to fertilize (Frolikova et al. 2018; Rubinstein et al. 2006).

The presence of CD81-positive vesicles was confirmed in bovine follicular fluid (**FF**), where Hung et al. (2015) found a correlation between tetraspanin levels depending on follicle size. Santonocito et al. (2014) also confirmed the presence of CD63 and CD81 exosomal markers in human FF. Both authors suggested that the cargo carried by exosomes in FF plays a role in stimulating follicle growth and cumulus expansion for further successful oocyte maturation. Later, clusters with CD81-positive vesicles were identified in human placenta (Burkova et al. 2018) as well as in PVS porcine (Jankovicova et al. 2019) and bovine (Jankovicova et al. 2016) embryos. It is assumed that the cargo with a specific proteome carried via exosomes during embryogenesis may be involved in fetal development and the maternal immune response (Burkova et al. 2018).

3.3.3 CD151

The CD151 tetraspanin is a common protein whose proteosynthesis has been detected in numerous tissue types and cells, including female oocytes. However, only recently, the presence of CD151 has been documented in human, bovine and mouse male gametes. Interestingly, as in the case of CD9, this protein was found in gametes at different maturation stages: spermatogonia, spermatids, testicular spermatozoa, and mature epididymal spermatozoa. In all the above-mentioned species, this protein is localized in the equatorial region of mature spermatozoa. Moreover, after AR, it is also present in their inner acrosomal membrane region. Surprisingly, unlike CD9 and CD81, CD151 is located in the same spermatozoa regions in all three species (Jankovicova et al. 2020a).

Depending on the glycosylation level, the molecular mass of CD151 can vary from 28 to 38 kDa. After the expression of CD151, it actively interacts with laminin-binding integrins such as α3β1 as well as with various variations of the α6 subunit (α6β1, α6β4) (Yang et al. 2012). By creating such complexes, it performs many functions, including those associated with successful fertilization. For example, Jankovicova et al. (2020) suggested that CD151/α6β4 can regulate actin cytoskeleton dynamics in spermatozoa and that CD151/α6β4/plectin could stabilize the equatorial domain of the spermatozoa during AR. The CD151/α6β1 patch organized by CD9 on the human oocyte and adding a CD151 antibody to the oocyte partially inhibits the effectiveness of gamete fusion. Because of that, it is suggested to be a part of the complicated gamete fusion complex (Ziyyat et al. 2006; Wolf et al. 2003).

Apart from the CD151 cis-interaction with sperm membrane integrins, it is also assumed that the CD151 interaction occurs with other integrins and tetraspanins in a trans-interaction. It helps to promote interactions between an egg and a spermatozoon. For example, CD151 and CD9 (oocyte) can interact with CD49 (sperm); CD49 and integrin α4 (sperm) can interact with CD63 and CD81 (oocyte), etc. (Sabetian et al. 2014; Jankovicova et al. 2020a).

Additionally, CD151 was detected on EVs from different origins, such as epididymosomes (Nixon et al. 2019). But particular attention was given to the vesicles containing CD151 in cancer research. A recent study by Brzozowski et al. (2018) has found that changes in CD9 and CD151 tetraspanin levels in vesicles can potentially lead to an

increase in the invasive and migratory ability of the non-tumorigenic prostate cell population. They also suggested that those changes could be potentially driving forces in prostate cancer metastasis. Another similar study was performed by Li et al. (2021) on the CD151 expression in exosomes in triple-negative breast cancer (**TNBC**). It was revealed that exosome samples from TNBC-positive patients had an increased expression of CD151 compared to the exosomal profile of healthy patients. These results could lead to the use of CD151 tetraspanin as a diagnostic biomarker for TNBC (Li et al. 2021).

3.3.4 CD63

Another equally important tetraspanin with a molecular weight of about 25 kDa is CD63, also known as Lysosome Associated Membrane Protein 3. Based on its full name, it is clear that this protein is expressed in lysosomes and associated endocytic organelles. It was also founded on cellular PM, but in smaller quantities (Latysheva et al. 2006; Pols & Klumperman 2008; Bassani & Cingolani 2012). CD63 is also well known for its direct interaction with the post-synaptic density protein/disc-large/zonulin I (**PDZ**) domain of Syntenin-1 (Latysheva et al. 2006). This PDZ domain attaches to the C-termininus of CD63 and plays a key role in organizing signalling complexes and holding tetraspanin network complexes together. The microdomains of this network most commonly include cholesterol, some types of integrins, and other tetraspanins (Pols & Klumperman 2008).

Often CD63 can be found as part of EVs. CD63-positive EVs were identified in boar SP (Alvarez-Rodriguez et al. 2019; Barranco et al. 2019), mouse (Nixon et al. 2019) and human epididymosomes (Thimon et al. 2008). However, the absence of this protein, despite its abundance in lysosomes and exosomes, does not lead to significant abnormalities. Schroder et al. (2009) confirmed normal fertility and viability in CD63 knockout mice and suggested that other tetraspanins could compensate for the lack of CD63.

The presence of CD63-positive vesicles was also identified in mare (da Silveira et al. 2012), bovine (Sohel et al. 2013), and porcine (Matsuno et.al 2019) FF. The CD63 and HSP70 positive signals were present in the uterine luminal fluid of pregnant ewes (Burns et al. 2014). Later a CD63 and CD9 positive vesicle population was also found in human (Giacomini et al. 2017) and bovine (Mellisho et al. 2017) embryos. The abundant variety of CD63-positive vesicles in mammalian reproductive fluids leads to the conclusion that CD63 contributes to the reproductive process. For example, da Silveira et al. (2017) noted that the embryo absorbs CD63-positive EVs produced from bovine FF during its early development. This author also suggests that these vesicles mediate the transfer of information from FF to the oocyte (da Silveira et al. 2017). Burns et al. (2014) assume that vesicles enriched with tetraspanins, including CD63, may mediate communication between the maternal endometrium and the conceptus trophectoderm in the preimplantation period.

3.4 Methods for EVs' isolation and analysis

The extensive study and practical application of EVs, especially exosomes, has led to increased demand for technically and economically affordable and efficient methods of vesicle isolation in medicine and science. However, despite the advances already made in

the field, there is still no consistent standardization of the isolation methods (Doyle & Wang 2019; Zarovni et al. 2015). Several reasons contributed to the problem with EVs' isolation. The first main reason is the high heterogeneity of the vesicles, which causes problems in the Isolation of specific types of vesicles. Another problem is the difficulty separating desired particles from impurities in the extracellular compartment. Finally, the quality of isolation is also affected by the specificity of physicochemical and biochemical properties of the biological fluids (Doyle & Wang 2019; Li et al. 2017). Therefore, several isolation methods for vesicles are based on different characteristics such as density, size, shape, and biochemical composition (Li et al. 2017).

Nowadays, a relatively large number of techniques are used in vesicle isolation. Nevertheless, few basic and most accessible are often used. These methods can be divided into three main techniques: ultracentrifugation, ultrafiltration, and immunoaffinity-based isolation. They could also be combined (Zhang et al. 2018).

For the isolation of reproductive fluids, ultracentrifugation is the most popular technique (Alvarez-Rodriguez et al. 2019; Alminana et al. 2017; Kupcova Skalnikova et al. 2019; Barranco et al. 2019), which is sometimes complemented by filtration (Zhang et al. 2020).

3.4.1 Ultracentrifugation techniques

Presently, ultracentrifugation can be considered a «gold standard» in exosome isolation techniques (Doyle & Wang, 2019; Zhang et al. 2018). There are several types of EVs' isolation. The best-known and most used are differential ultracentrifugation (**dUC**) and density gradient ultracentrifugation (**DGUC**).

The main principle of dUC is the separation of small particles in the suspension based on their size, density, and shape. The rotation of a rotor creates a centrifugal field that separates the particles. The forces it creates are several orders of magnitude greater than gravity. The result of each cycle is the successive separation and sedimentation of larger and denser particles (see **Fig. 5**). It is possible to optimize the isolation protocol for the specific vesicles by adjusting a number of steps. (Li et al. 2017; Livshits et al. 2015).

The dUC is the most affordable technique because it does not require additional sample preparation or special kits (Zhang et al. 2018; Li et al. 2017). However, this method has its disadvantages. Different types of EVs often have similar sedimentation properties. As a result, this could lead to contamination of isolated exosomes and a low yield. In addition, excessively long and intensive dUC (>4 hours) causes mechanical damage to the exosomal membrane and increases protein aggregates contamination in the sample (Cvjetkovic et al. 2014). From the technical point of view, using different types of rotors across studies, an identical protocol can result in slightly different outcomes (Livshits et al. 2015).

DGUC works on a similar principle/way as dUC. However, this method separates particles by adding a gradient (sucrose or iodoxinol) to a centrifuge tube under the supernatant. During DGUC, a sample with exosomes is carefully placed onto the surface of the gradient. The density of a gradient decreases from bottom to top. Due to centrifugal force, exosomes are grouped and move across the gradient in a direction closer to the bottom of

the tube. In the end, exosomes form a separate layer, which can then be collected in fractions (Li et al. 2017; Zhou et al. 2020).

This method is more accurate than dUC. It helps to separate the exosomes from other types of EVs more carefully and avoid protein aggregates contamination. However, DGUC is not able to divide exosomes from viruses or some MVs. This method is additionally time-consuming and might take from 16 to 20 hours (Li et al. 2017; Zhang et al. 2018).

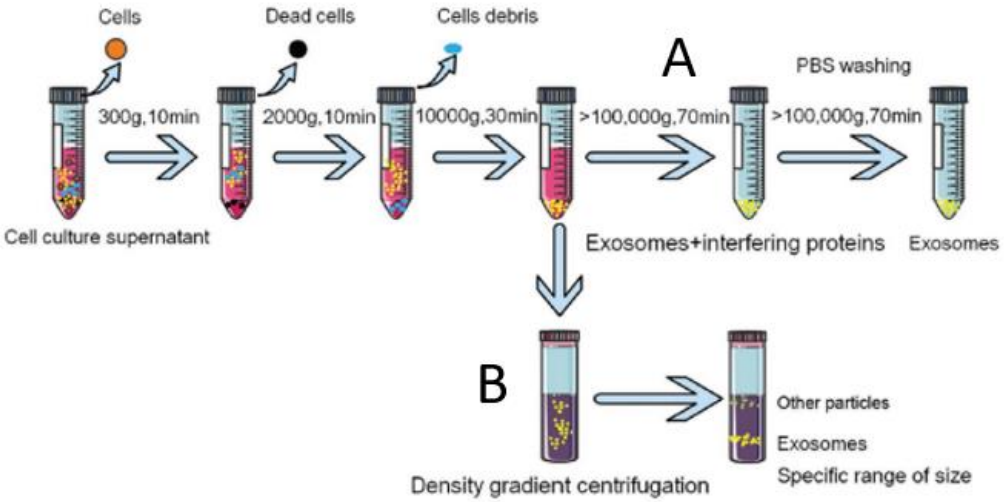

Figure 5: Schematic representation of the basic principles of differential (**A**) and density gradient (**B**) ultracentrifugation techniques by *Zhang et al. (2018)*.

3.4.2 Ultrafiltration or size-based techniques

Based on EVs' size and molecular weight, ultrafiltration (**UF**) is also performed as an exosome isolating technique. This method is based on adding the supernatant in columns with special semipermeable membrane filters with a molecular weight and pore diameter of about 0.1-0.22 μm (Zhou et al. 2020). The molecular weight cut-off is performed under centrifugal force. While a filter traps large molecules, small exosomes pass to the filtrate through the membrane (Li et al. 2017; Zhang et al. 2018).

Compared to ultracentrifugation, the reduced time-consuming of the UF technique is a great advantage. The UF also does not require expensive equipment. However, this method is not precise and does not qualitatively isolate exosomes from the rest of the EVs and plasma proteins (Li et al. 2017; Doyle & Wang, 2019).

3.4.3 Immunoaffinity capture-based techniques

The next type of exosome isolation method is immunoaffinity capture-based techniques (**IA**). IA is based on the identification (capturing) of membrane proteins that are

expressed on exosomes. The most popular IA techniques are the enzyme-linked immunosorbent assay (**ELISA**) and magneto-immunoprecipitation.

ELISA is based on the principle of exosome capture using antibodies immobilized on a microplate (96 wells in 100 µl), which attach to the antigen on the surface of the exosomal membrane. Among biomarkers for the detection and isolation of exosomes, the previously mentioned and described family of tetraspanin proteins, as well as Alix, annexin, Rab5, and epithelial cell adhesion molecule (**EpCAM**) are often used (Zhang et al. 2018). However, a big disadvantage of this technique is the importance of antigen expressing on the surface of the exosomal membrane, because the antibody is not able to recognize the antigen inside the dense lipid bilayer (Li et al. 2017).

The next quite popular IA method is magneto-immunocapture. In this technique, a specific for exosomal markers biotinylated antibody is attached to streptavidin-coated magnetic beads. Later, the beads with the antibody are incubated with the sample to further isolate the desired exosome population. Due to the larger trapping area, magnetic beads provide better isolation (Doyle & Wang 2019).

In comparison with ultracentrifugation, the big advantage of IA is the possibility to isolate a higher concentration of intact exosome populations using a smaller volume of the starting product, which makes the magnetic immunoprecipitation method especially useful. Also, IA methods have a benefit in isolating exosomes from viscous and complex fluids such as plasma (Zarovni et al. 2015). In practice, however, it is more common to combine ultracentrifugation and IA to improve the quality of EVs isolation (Mathivanan et al. 2010).

4 Materials and methods

4.1 Materials

4.1.1 Raw material

In those experiments, a spermatozoa and SP of a domestic pig (*Sus scrofa domesticus*) were used as an object of study.

Boar sperm fraction of Duroc breed was taken from insemination station Skrsin (Liprapork, s.r.o., Czech Republic). Fresh ejaculate was processed immediately, semen insemination doses were stored in a refrigerated thermobox at 17 °C and processed the day after collection.

4.1.2 Set of antibodies

4.1.2.1 Primary antibodies

- Rabbit polyclonal anti-CD9 (MRP-1): bs248902, (Bioss Inc, USA). Dilution with PBS at a ratio 1:250.
- Rabbit polyclonal anti-CD151: bs-2524r (Bioss Inc). Dilution with PBS at a ratio 1:250.
- Rabbit polyclonal anti-CD81 (H-121): sc-9158 (BioTech, USA). Dilution with phosphate-buffered saline (PBS) at a ratio 1:250.
- Mouse monoclonal anti-CD63 (MEM-259): MA1-19281 (Invitrogen, USA). Dilution with PBS at a ratio 1:250.
- Rabbit monoclonal recombinant anti-integrin alpha V: ab179475 (Abcam, USA) 1:500
- Rabbit polyclonal anti-BHB3 (AQN), anti-BHB7 (AWN) spermadhesins (Jonakova et al. 1998); anti-PSP1 spermadhesin (Manaskova et al. 2008) (Produced by laboratory of Biochemistry of Reproduction; Institute of molecular genetics CAS; Prague). Dilution with PBS at a ratio 1:10,000.

4.1.2.2 Secondary antibodies

- Anti-R (anti-rabbit): a goat anti-Rabbit IgG (H+L) is conjugated to horseradish peroxidase (HRP) (Bio-Rad, USA). Dilution with PBS at a ratio 1:3000 for tetraspanins detection. Dilution with PBS at a ratio 1:6000 for spermadhesin detection.
- Anti-M (anti-mouse): a goat anti-Mouse IgG (H+L) is conjugated to horseradish peroxidase (HRP) (Bio-Rad). 1:3000 dilution.
- Anti-M Alexa FluorTM 488 (Invitrogen). 1:300 dilution.
- Anti Rat Alexa FluorTM 488 (Invitrogen). 1:300 dilution.
- Anti R Alexa FluorTM 488 (Invitrogen). 1:300 dilution.

4.2 Methods

4.2.1 Extracellular vesicles isolation from seminal plasma

4.2.1.1 Centrifugation

For better exosome isolation from SP, the ejaculate was cleaned from sperm pellets and other undesirable debris. Therefore, the first three cycles of separation took place in a Centrifuge 5804R (Rotor A-4-44, Eppendorf, Germany). Centrifugation of ejaculate at 25°C for 10 min at 300 × g. The supernatant was transferred into the new tube. Centrifugation of supernatant at 25°C 10 min at 2000 × g. The supernatant was transferred into the new tube. Centrifugation of supernatant at 4°C 30 min at 10,000 × g. The supernatant was transferred into new tube.

4.2.1.2 Differential ultracentrifugation

Samples were transferred into Beckman Coulter™ Ultra-Clear Centrifuge Tubes. The tubes were then filled to the edge with saline solution (0.9% NaCl), weighed, equilibrated and placed in the rotor. Ultracentrifugation was performed at 4°C for 70 min and at 100,000 × g (acceleration max. 0; deceleration max. 0). The supernatant was then aspirated to leave a few milliliters at the bottom. The pellets were resuspended in the supernatant and diluted with a new portion of saline. The centrifuge tubes were equilibrated for the second centrifugation under the same conditions (4°C, 70 min, 100,000 × g). The supernatant was carefully removed, and the pellets were resuspended in saline solution and stored at -20°C until further use. Ultracentrifugation was performed on a Beckman Coulter Optima XPN-90 ultracentrifuge (SW40Ti rotor, Beckman Coulter, USA).

4.2.1.3 Density gradient ultracentrifugation

The first two steps of DGUC were almost the same as for dUC with minor changes. For DGUC, samples were resuspended in PBS (7-10 ml). Ultracentrifuge tubes (Beckman Coulter™ Ultra-Clear Centrifuge Tubes) were equilibrated and placed into the rotor (SW40Ti, Brea, California, USA). The centrifugation of the samples was performed in two runs under the same conditions (4°C, 70 min, 100,000 × g, [acceleration max. 0; deceleration max. 0]) on a Beckman Coulter Optima XPN-90 ultracentrifuge. Between the runs, the supernatant was removed, and the pellets were reconstituted with fresh PBS. After the second run, the pellets were resuspended in fresh PBS (7-10 ml) for the next step.

To perform gradient ultracentrifugation, tubes containing sucrose gradient were prepared. For that, the tubes were filled out with 30% sucrose solution (9 ml), and the pellet suspension was carefully placed on top of the gradient. Each tube was equilibrated by topping it with PBS solution. The run was performed at 4°C for 2 h at 75,000 × g (acceleration 7; deceleration 5).

The tubes were separated into 2 types. The first type (2 tubes) – the supernatant was aspirated and remaining EVs were filled with PBS. The second type (4 tubes) – the sucrose

with pellets was pipetted into tubes and filled with PBS. Another ultracentrifugation was accomplished under 4℃ for 35 min, and 100,000 × g (acceleration max. 0; deceleration max. 0) conditions. The supernatant was aspirated, and the remaining pellets were resuspended and moved into new Eppendorf Microcentrifuge Tubes (2.0 ml). Tubes with pellets were diluted with PBS and stored at -20℃ until use.

4.2.1.4 Filtration

Purified SP was transferred into Nanosep Centrifugal Devices with Omega™ Membrane 300K tube (PALL, USA). Centrifugation ran under at 25℃ for 2-3h, and 5000 × g conditions until supernatant passed through the filter membrane, and EVs stayed on it. The supernatant was aspirated, and the PBS (200 µl) was added to the filters with EVs. Second centrifugation was accomplished with the same conditions (25℃, 2-3h, 5000 × g). The supernatant was aspirated, and isolated EVs were diluted in the PBS (50 µl).

4.2.1.5 Transmission electron microscopy (TEM)

For the samples preparation for TEM, two types of solution were made:

1. HEPES type: 25 mM Trehalose dihydrate (Sigma-Aldrich) diluted in 1M HEPES (Sigma-Aldrich) × (5 ml) dH2O pH 7.4.
2. Saline type: 25 mM Trehalose dihydrate diluted in (5ml) Saline solution (0.9% NaCl).

The pellets from dUC were resuspended in (800 µl) HEPES and saline solutions. The 400 µl of each solution was ready for TEM. Negative staining was taken as a sample preparation method. The ample solution was adsorbed to a copper grid and stained with a solution of heavy metal salts. TEM images were prepared on the core facility: Imaging Methods Core Facility at BIOCEV (IMCF).

4.2.1.6 Protein isolation

4.2.1.6.1 Protein isolation with 100 mM NaOH (basic conditions)

The vesicles were diluted with NaOH (100 mM) at a ratio of 1:2 (lysates:NaOH) and incubated at 4℃ overnight while shaking. The suspensions were sonicated 3 times for 15 s with 1 min pause. After each sonication, the samples were cooled on ice for about 1 min. After the centrifugation at 4℃ for 15 min at 7000 × g, acetone was aspirated:

- A reducing buffer (30-200 µl) (0.5 M Tris-HCl, glycerol, 10% SDS; 2-mecraptoethanol) was added to the pellets. The resulting samples were vortexed, incubated at 95℃ for 5 min while shaking and prepared for electrophoresis.
- A non-reducing sample buffer (0.5 M Tris-HCl, glycerol, 10% SDS) was added to the sample. The resulting mixture was incubated at 95℃ for 5 min while shaking. Samples were used for the MS in the core facility Centre of Molecular Structure.

4.2.1.6.2 Protein isolation with RIPA buffer in acidic conditions

The vesicles were diluted at a ratio of 1:1 with the RIPA buffer. The samples were incubated on ice for 10 min and sonicated 3 × 10 min (10 sec sonication and 1 min rest on ice). Samples were centrifugated at 4℃ for 10 min at 14,000 × g. The supernatants were transferred into new tubes. TCA was added to the samples at a 1:4 ratio. Lysates were incubated on ice for 10 min and centrifugated at 4℃ for 5 min at 14,000 × g. Supernatants were aspirated, and acetone (200 µl) was added to the pellets. The samples were centrifugated at 4℃ for 5 min at 14,000 × g. Acetone washing was repeated two times until pellets were free of TCA. Acetone was aspirated:

- A reducing buffer with urea (8M Urea; 0.5 M Tris-HCl, glycerol, 10% SDS; 2-mercaptoethanol) (30-200 µl). Samples were vortexed, incubated at 95℃ for 5 min while shaking and prepared for electrophoresis.
- A non-reducing sample buffer for SDS electrophoresis (0.5 M Tris-HCl (Bio-Rad), glycerol, 10% SDS) (100 µl). The resulting mixture was incubated at 95℃ for 5 min while shaking. Samples were used for the MS.

4.2.1.7 Super-resolution microscopy

Centrifugated by dUC vesicle pellets were resuspended in saline solution with 25 mM trehalose, the Lipophilic Styryl dye FM4-64Fx (5 mM) was applied to the saline solution with vesicles at a ratio 1:100 and incubated overnight at 37 ℃. On the next day, samples were centrifugated at 4℃ for 70 min and 100,000 × g (acceleration max.; deceleration max.). The supernatant was aspirated, and pellets were resuspended and stored in the dark space until sperm pellets preparation.

In the meantime, sperm fraction was centrifugated at room temperature (**RT**) for 5 min and 300 × g and 3 times washed in saline solution. The supernatant was aspirated, and sperm pellets were resuspended in (200-400 µl) mHTF buffer [NaCl (0.571 g); KCl (0.0349 g); KH2PO4 (0.005 g); CaCl (0.0226 g); 5 mM HEPES (0.1192 g); Sodium pyruvate (0.0036 g); sodium lactate (181.68 µl); gentamicin (100 µl)]. Sperm motility and concentration were calculated by software Computer-Assisted Sperm Analysis (CASA) (ISAS Motil 2008; Proiser R+D Systems). (v. 1.2; Proiser, Spain).

Sperm pellets were co-incubated with EVs for 3 h at 37℃ in HTF medium. For the control group sperm pellets without EVs co-incubation were used, and sperm were stained with dye FM4-64Fx. Post-incubation samples were washed (3 × 300 g, 5 min) in saline solution. Samples (10 µl) were applicated on microscope cover glass slides and fixed with 3,2% paraformaldehyde (70 µl) and after 7 min of incubation slides were carefully washed with saline solution. The SuperBlock medium (Blocking Buffer in PBS; Thermo Fisher Scientific) was applicated on the cover glass slides, and samples were incubated for 30 min. The cover glass slides were then washed with saline. After blocking, part of cover glass slides with spermatozoa with EVs was incubated with lectin PNA, Alexa FluorTM 488 conjugate (Invitrogen), diluted at a ratio 1:1000, 60 min at RT. Cover glasses with and also without PNA lectin, and cover glass slides with control samples were incubated with DAPI diluted in saline at a ratio 1:500 (DAPI:saline) for 5 min in the dark, then washed in saline, and at the end the slides were washed in dH2O, and air-dried. Then the dry samples were

mounted with a mounting medium (90% glycerol with 5% anti-fade N-propyl gallate). The super-resolution images were obtained by DeltaVission OMX™ V4 (Light Microscopy Core Facility, IMG CAS, Prague, Czech Republic).

4.2.1.8 Immunofluorescent Detection of tetraspanins

Cover glass slides with fixed sperm with stained EVs by 3,2 % PFA were washed in saline solution and incubated in the Superblock buffer for 30 min at RT. Then the samples were washed and incubated with primary antibodies (anti-CD9 antibody, anti-CD151 antibody, anti-CD81 antibody and anti-CD63 antibody) overnight, at 4 °C. On the next day, the slides were washed with saline solution and the slides were incubated for 60 min at RT with secondary antibodies (Alexa Fluor 488, Invitrogen, Waltham, MA, USA) diluted at a ratio 1:300 in saline solution. After incubation, the slides were washed is a saline solution and incubated with DAPI diluted in saline at a ratio 1:500 (DAPI:saline) for 5 min in the dark, then washed in saline, and at the end, the slides were washed in dH2O, and air-dried. Then the coverslips dry samples were mounted with a mounting medium (90% glycerol with 5% anti-fade N-propyl gallate).

The Multi-color SIM super-resolution images were obtained by DeltaVision OMX V4 (Light Microscopy Core Facility, IMG CAS, Prague, Czech Republic).

4.2.1.9 Sodium dodecyl sulfate–polyacrylamide gel electrophoresis (SDS PAGE)

Composition of reagents:

Separation gel (12%)

- (3.5 ml) dH2O
- (2.5 ml) 1,5 M Tris-HCl Resolving buffer pH 8.8 (Bio-Rad)
- (4 ml) 30% Acrylamide/Bis solution (Bio-Rad)
- (100 µl) 10% SDS (Bio-Rad)
- (4.5 µl) TEMED (Sigma-Aldrich)
- (70 µl) 10% Ammonium persulfate (APS; Sigma-Aldrich), aq. solution

Stacking gel (4%)

- (1.52 ml) dH2O
- (625 µl) 0,5 M Tris-HCl Stacking buffer pH 6.8 (Bio-Rad)
- (325 µl) 30% Acrylamide/Bis solution (Bio-Rad)
- (25 µl) 10% SDS (Bio-Rad)
- (3.8 µl) TEMED (Sigma-Aldrich)
- (50 µl) 10% APS (Sigma-Aldrich)

Electrode buffer (2 l)

- (200 ml) 10 × Electrode buffer (Tris, 60.6 g; Glycine, 288 g; SDS, 20 g)
- (2 l) dH2O

Separation of proteins was made with the SDS-PAGE electrophoresis method using acrylamide gel. A separation/resolving gel with 12% density was used for proteins with a sufficiently small molecular mass (20-35 kDa). The gel was poured between two glass

panels and subsequently recoated with dH2O for 30 min. Meanwhile, a 4% stacking gel was prepared. After the separation/resolving gel polymerized, dH2O was poured out and stacking gel was added on top of the resolving gel. The combs were immediately inserted. The gel was incubated for 15 min before use. The glass panels coated with gel were placed in a tank containing an electrode buffer. Molecular protein standard Precision Plus Protein Standards Dual Color (Bio-Rad) was used in a separate well to distinguish molecular weights. Electrophoresis was performed at 80 V constant voltage for the first 20 min, and at 140 V constant voltage for the next 90 min. After the protein separation, the gel was prepared for Western blot or Coomassie staining.

A vertical mini gel electrophoresis system Mini-PROTEAN Tetra Cell and PowerPac 1000 (Bio-Rad) was used.

4.2.1.10Western blot

To perform a semi-dry Western blot, the Trans-Blot TurboTM transfer system (Bio-Rad) was used. Before the run, filter papers (Cytiva, USA) (8 pcs), polyvinylidene difluoride (PVDF, Merck Millipore, USA) or nitrocellulose (NC; Merck Millipore) membrane sheets, transfer buffer and the gel cassette were prepared. The transfer buffer was made freshly by mixing 5 × Trans-Blot TurboTM transfer buffer (200 ml) with dH2O (600 ml) and 96% ethanol (200 ml).

Filter papers and NC membrane were soaked in a transfer buffer for 5 min. In case of using a PVDF membrane, it was firstly activated by soaking in methanol for 1 min and then transferred into a blotting buffer. Meanwhile, the gel was carefully removed from glass panels, briefly washed in dH2O for 5-15 s and placed on the membrane. The cassette stack was organized in the following order starting from the bottom anode tray: four filter papers, membrane, gel, and four filter papers. All air bubbles were removed with a blotting roller. Afterwards, the cassette was locked with the top cathode lid. The blotting was performed on a low molecule weight program for 10 min.

After the blotting, the membrane was washed in dH2O for about 10 s and stained for 1 min in Ponceau S solution (Sigma-Aldrich). The membrane background was washed away with dH2O before it was imaged. The remaining Ponceau was removed from the membrane by incubating it in 0.5% PBS Tween 20 pure (SERVA, Germany).

4.2.1.11Immunodetection

The membrane was placed into the solution of non-fat dry milk (ChemCruz, USA) (2.5 g) in PBS (50 ml) and incubated for 1 h at RT while shaking. After blocking, the membrane was incubated with 0.5% PBS-T solution (3 × 15 min). The membrane was then placed in the primary antibody solution (PBS, 1 ml; primary antibody) and incubated at 4°C overnight. The next day, the membrane was washed with 0.5% PBS-T solution (3 × 15 min) before incubation with the secondary antibody solution (PBS; secondary HRP-linked antibody) at RT for 1 h. After incubation with the secondary antibody, the membrane was washed with 0.5% PBS-T solution (3 × 15 min).

To perform chemiluminescent visualization, the chemiluminescent western blotting SuperSignal West Femto Maximum Sensitivity substrate (Thermo Scientific) was distributed on a membrane before it was scanned with Azure c300 Gel Imaging System (Azure Biosystems, USA).

5 Results and Discussion

5.1 Results

5.1.1 EVs isolation

For the successful evaluation and characterization of EVs extracted from boar SP, the enrichment protocol based on the ultracentrifugation techniques was implemented as the first step in the current study. To isolate EVs fraction from raw material, two different approaches to separation have been conducted. These are dUC and DGUC with sucrose as a gradient. dUC resulted in transparent gel-like pellets containing EVs (see **Fig. 6**, indicated by arrows). However, DGUC results did not show any presence of such pellets.

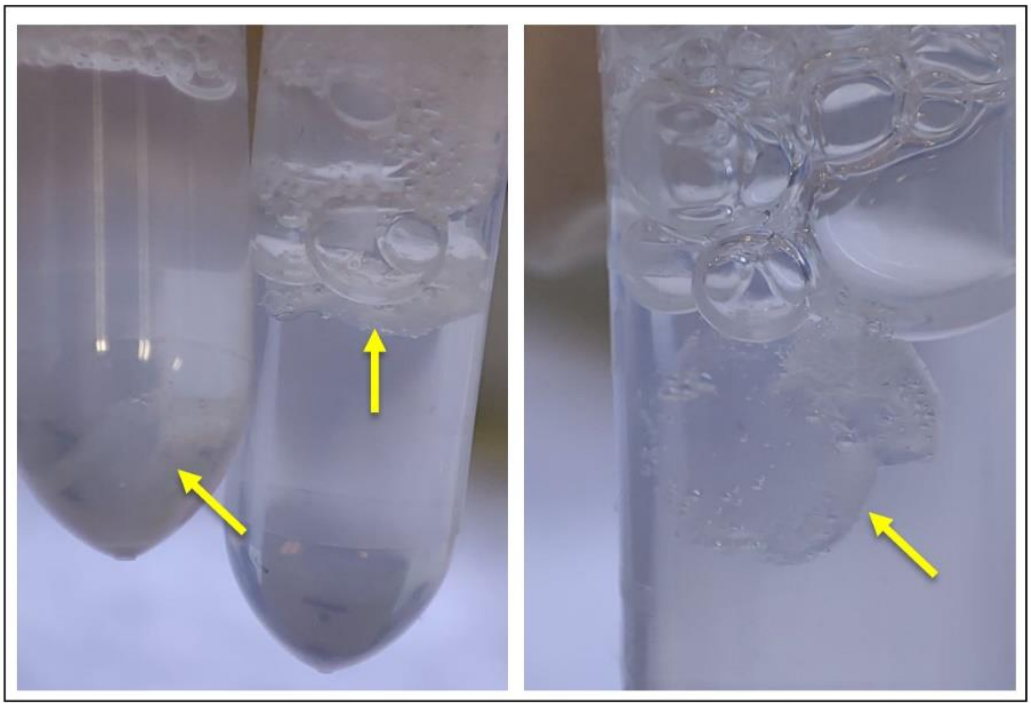

Figure 6: Pellets containing EVs after a dUC performing. Yellow arrows show a pellet.

The resulting pellets were collected and subsequently used for the preparation of TEM samples to visually approve the presence of EVs. Vesicles and multivesicular bodies of different shapes and sizes were detected. The TEM sample prepared with HEPES buffer contained uniform and separated vesicle structures from 20 to 500 nm in diameter that correspond to EV's morphology (see **Fig. 7**). The saline-based sample contained rather irregular-shaped vesicular agglomerations or multivesicular bodies including individual vesicle structures (see **Fig. 8**, red arrow), which could be possibly caused by high salt concentration.

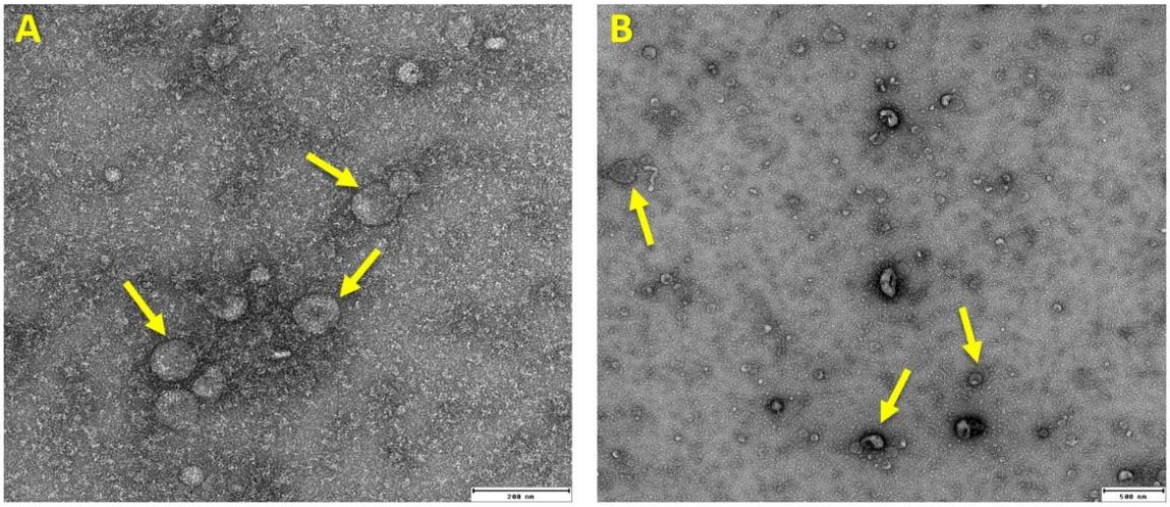

Figure 7: Isolated EVs in HEPES type solution using TEM. Yellow arrows show an isolated vesicles. **A** – 200 nm resolution; **B** – 500 nm resolution.

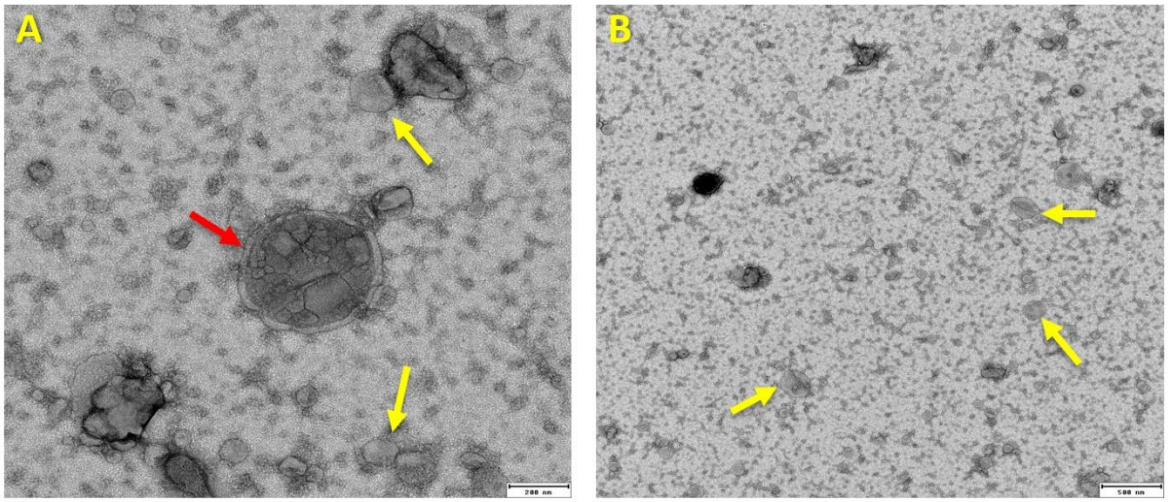

Figure 8: Isolated EVs in saline-type solution using TEM. Yellow arrows show isolated vesicles, red arrow – multivesicular agglomeration. **A** – 200 nm resolution; **B** – 500 nm resolution.

5.1.2 Proteomic study of EVs

The pellet fraction was further subjected to an MS-based analysis to confirm the presence of EV-specific proteins. Samples were prepared under basic and acidic conditions. The total amount of identified proteins was 42 and 35 for acidic and basic samples respectively with an overlap of 22 proteins that are common for both samples. The number of unique proteins identified only in acidic samples was 20, and 13 for basic conditions (see **Fig. 9**).

The spermadhesin protein family, which includes AQN, PSP1, and AWN proteins, was the main group of proteins identified with high confidence and accuracy among the 22 overlapping proteins. Each member of this family had a considerable number of identified peptides, with a significant number of unique peptides present in both acidic and basic conditions (**Tab. 1 and 2**). Moreover, the identified peptides covered a substantial portion

of the respective protein amino acid sequence. Along with extensive proteome coverage, the presence of the spermadhesins was also supported by the high signal intensities of peptides.

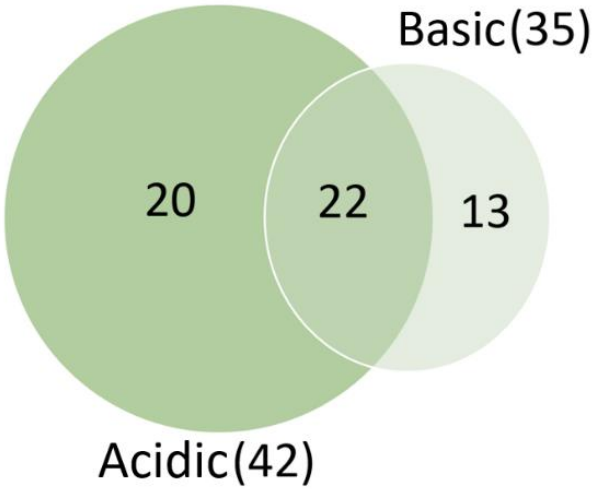

Figure 9: Venn diagrams of the total amount of proteins identified by MS. Acidic conditions – total amount of identified proteins was 42; with acidic isolation method was identified 20 unique proteins. Basic conditions – total amount of identified proteins was 35; with basic isolation method was identified 13 unique proteins. Total number of overlapping proteins between two isolation methods was 22.

The spermadhesin protein family, which includes AQN, PSP1, and AWN proteins, was the main group of proteins identified with high confidence and accuracy among the 22 overlapping proteins. Each member of this family had a considerable number of identified peptides, with a significant number of unique peptides present in both acidic and basic conditions (**Tab. 1** and **2**). Moreover, the identified peptides covered a substantial portion of the respective protein amino acid sequence. Along with extensive proteome coverage, the presence of the spermadhesins was also supported by the high signal intensities of peptides.

Apart from spermadhesins, other protein classes were found, such as cytoskeletal proteins (actin, tropomyosin) or proteases (hydrolases, glycosidases, serine and cysteine proteases) (see **Fig. 10** and **Tab. 1** and **2**). The distribution of protein classes was almost comparable for acidic and basic isolation conditions with a higher distribution of spermadhesins for acidic conditions (Ac) - 14%, than for basic conditions (Bc) - 21%. Distribution of cytoskeletal proteins was higher for basic conditions - 21% (Bc) and 14% (Ac). On the other hand, there we found more proteins related to such protein classes as proteases (17% - Ac, 14% - Bc), transfer proteins (12% - Ac, 7% - Bc), and chaperones (10% - Ac, 0% - Bc) under acidic conditions.

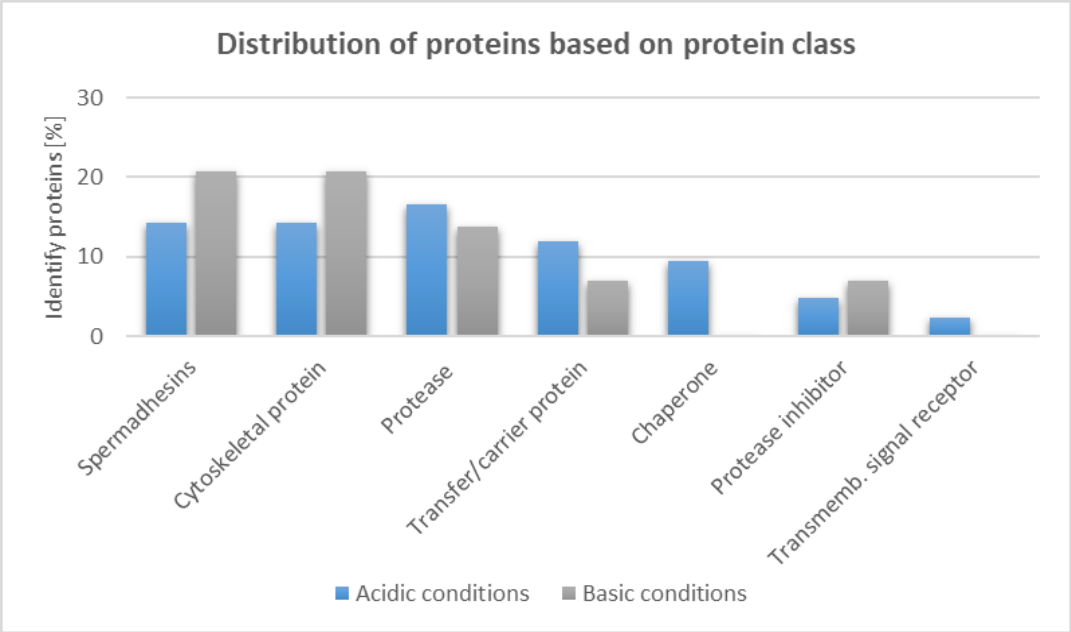

Figure 10: Protein class distribution identified proteins in seminal plasma EVs. Blue bars are corresponding to acidic conditions, grey basic conditions. Horizontal axes – the types of protein classes found in EVs samples. Vertical axes – percentage of identified proteins.

In terms of localization, the majority of proteins found both in the acidic and basic samples were identified as cytoplasmic proteins – 71% (Ac) and 66% (Bc). The next significant group of proteins was extracellular proteins - 55% (both Ac and Bc), followed by plasma membrane proteins - 45% (Ac) and 34% (Bc) (**see Fig. 11**).

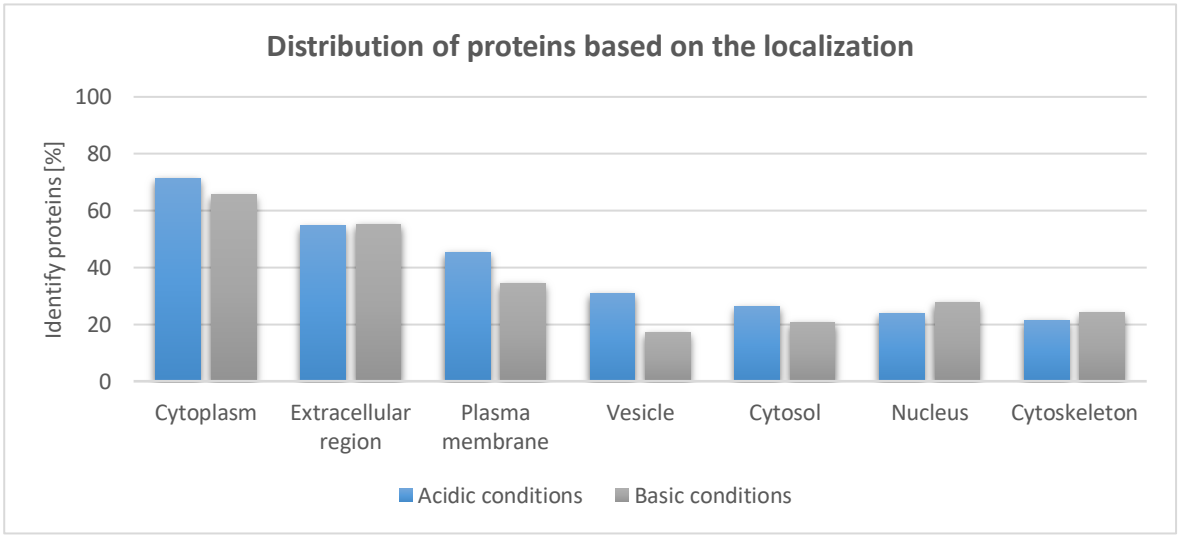

Figure 11: Distribution of identified proteins in seminal plasma EVs based on the localization. Horizontal axes – the types of processes in which proteins are involved. Vertical axes – percentage of identified proteins.

Regarding the function of proteins, the majority were found to be involved in biological, cellular, and metabolic processes, as shown in **Fig. 12**. In the scope of the current

thesis, the most relevant biological processes are reproduction and transport – EVs proteins actively promote current functions. There were found 31% (Ac) and 38% (Bc) of proteins participated in reproduction, and 36% (Ac) and 24% (Bc) of proteins related to the transport function. These findings, based on the current gene ontology analysis highlighting the distribution of proteins based on their class, localization, and functions, support the statement that the fraction obtained via dUC indeed contains EVs.

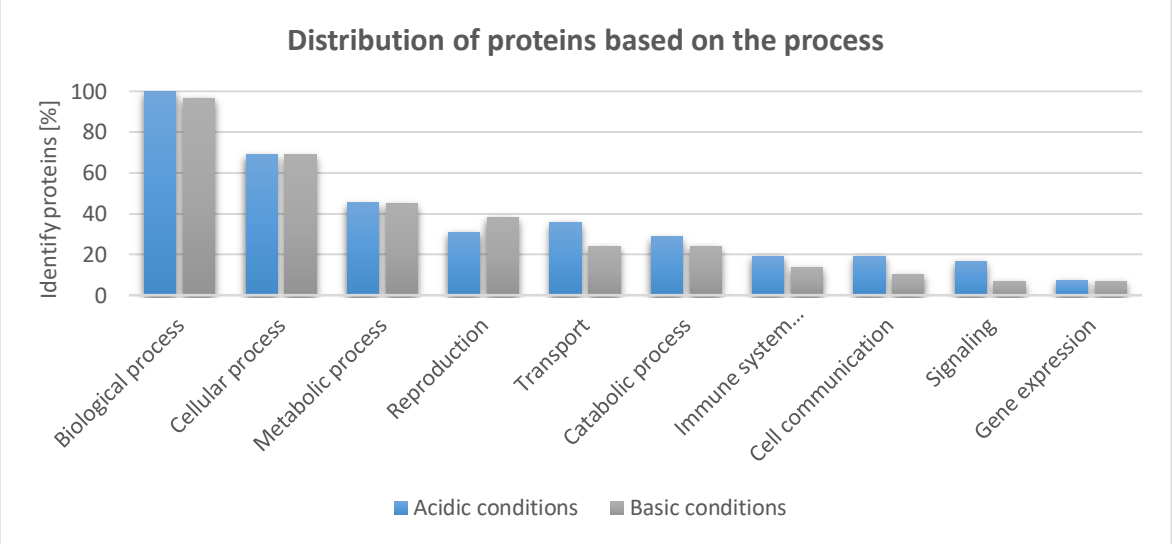

Figure 12: Distribution of identified proteins in seminal plasma EVs based on processes in which proteins are involved. Horizontal axes – the types of processes in which proteins are involved. Vertical axes – percentage of identified proteins.

5.1.3 Interaction of isolated EVs with boar spermatozoon

For the capturing visualization of interaction EVs with the spermatozoa, EVs have been isolated and stained in the Lipophilic Styryl dye FM4-64Fx EVs and co-incubated with spermatozoa stained in DAPI. In **Fig. 13**, it is clearly visible that the EVs (in red) interacted with all parts of the spermatozoa (head, neck, midpiece and tail). A stronger interaction was observed at the acrosomal and tail regions, where larger vesicles (white arrows) appear in higher numbers and form some sort of aggregation. It can also be seen that the vesicles were fused with the sperm membrane without penetrating the nuclei.

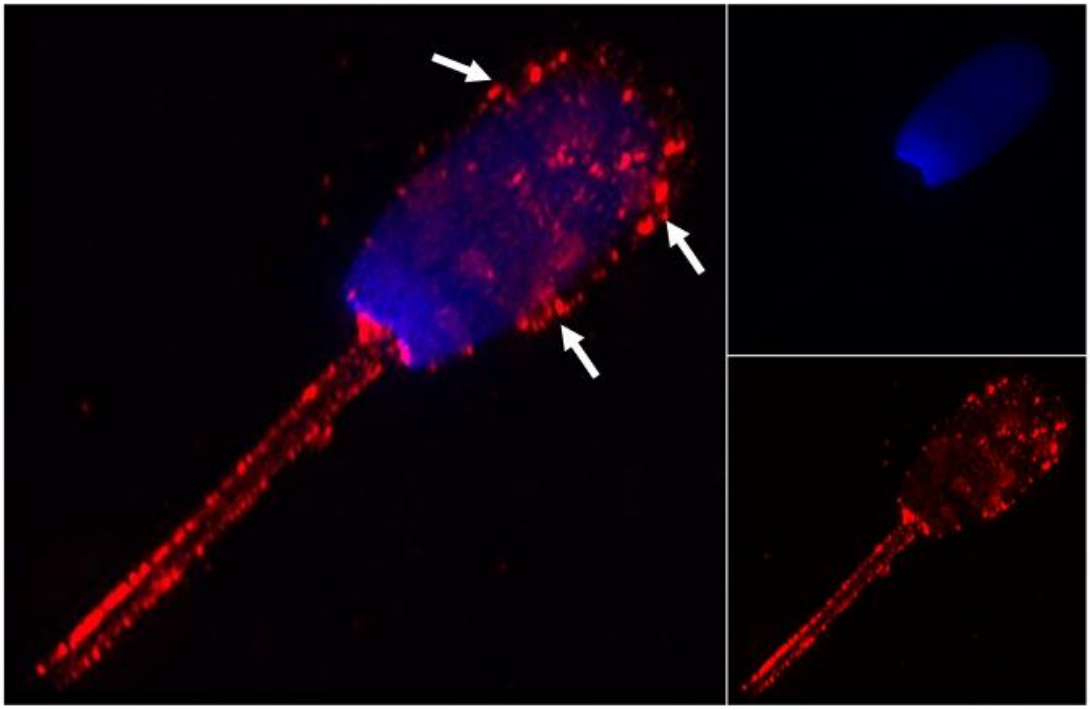

Figure 13: The co-incubated sEVs (red) with boar spermatozoon (blue) interaction visualization. Captured by Dr. M. Frolíková at the Imaging Core Facility at the Institute of Molecular Genetics, CAS, Prague.

5.1.4 Protein detection of isolated EVs

5.1.4.1 Protein profile of sEVs

The obtained exosomal pellets after DGUC, filtration and dUC were then subjected to SDS gel electrophoresis and subsequent Coomassie blue staining. Proteins were isolated in two different conditions. Basic conditions were applied to all the above-mentioned EVs isolation techniques. Whereas for dUC, there were applied basic and acidic conditions.

The DGUC and post-filtration residue (**Pf**) had similar results and showed no presence of any protein bands. As the opposite, the filtration (**Fc**) and SP showed so high protein concentration, that it was not possible to observe particular bands (see **Fig. 14A**).

Several protein bands were found in acidic and basic conditions after dUC (see **Fig. 15B**). Clearly distinguishable bands were observed in two molecular weight groups: the group of 13-15 kDa and the second group of several distinct bands appeared between 42 and >249 kDa. There was also one obvious band in both samples that corresponded to around 24-26 kDa

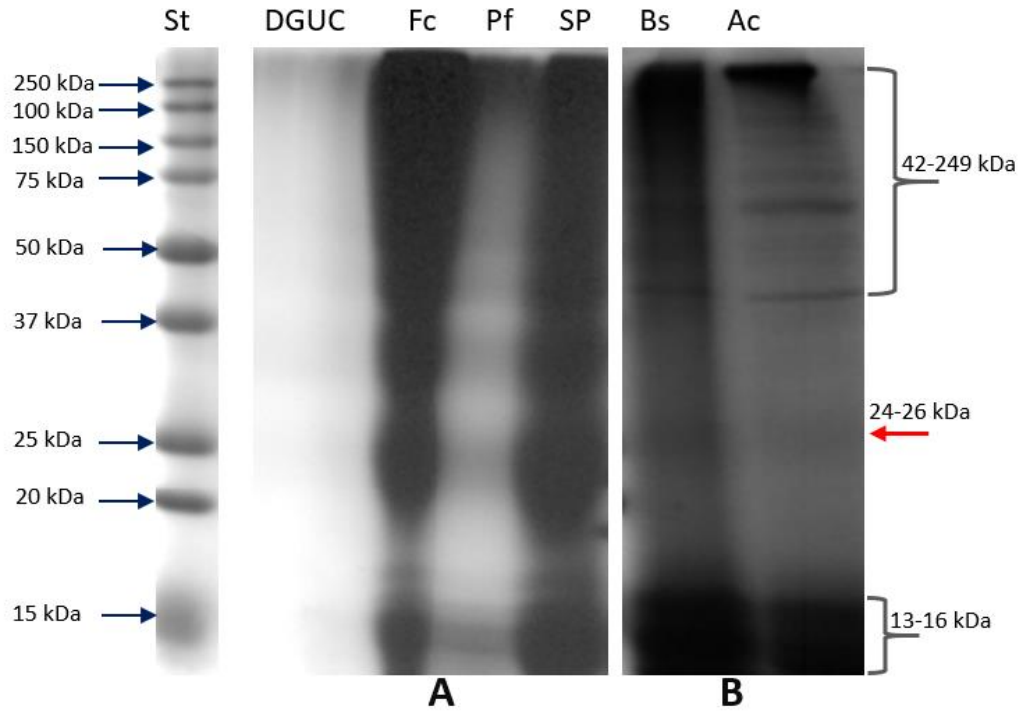

Figure 14: Coomassie blue staining of proteins obtained after DGUC/ filtration (**A**) and dUC (**B**) methods. St – molecular standard, DGUC – 3 samples from density gradient ultracentrifugation, Fc – filtration with collected exosomes, Pf – post-filtration residue, SP – purified seminal plasma, Bs – basic conditions (NaOH), Ac – acidic conditions (TCA).

5.1.4.2 Detection of selected proteins in isolated EVs from seminal plasma

To detect proteins of the tetraspanin, spermadhesin and integrin families, immunochemical methods were employed. Specifically, four antibodies targeting the tetraspanin family (CD9, CD151, CD81 and CD63), three antibodies targeting spermadhesins (AQN, AWN, PSP1) and one antibody targeting integrin alpha V were used to detect these selected proteins as EVs' markers in fractions obtained through dUC, DGUC or filtration under varying conditions.

The reducing basic conditions were applied for the samples after all three types of EVs' isolation. The above-mentioned members of the tetraspanin family were used as markers to confirm the presence of EVs in the samples. The immunodetection technique followed by chemiluminescent visualization was employed for this purpose. **Fig. 15** shows membranes incubated with antibodies to CD9, CD151, CD81 and CD63 tetraspanins and with negative control. Despite several unspecific bands (grey arrows), there are no specific bands found in these immunodetections.

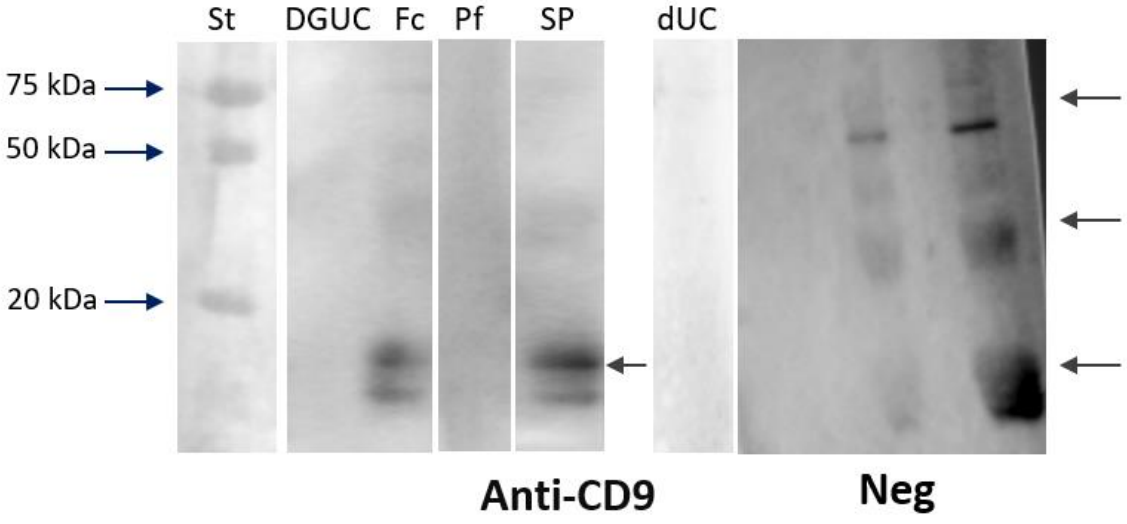
St
DGUC
Fc
Pf
SP
dUC
75 kDa
50 kDa
20 kDa
Anti-CD9
Neg

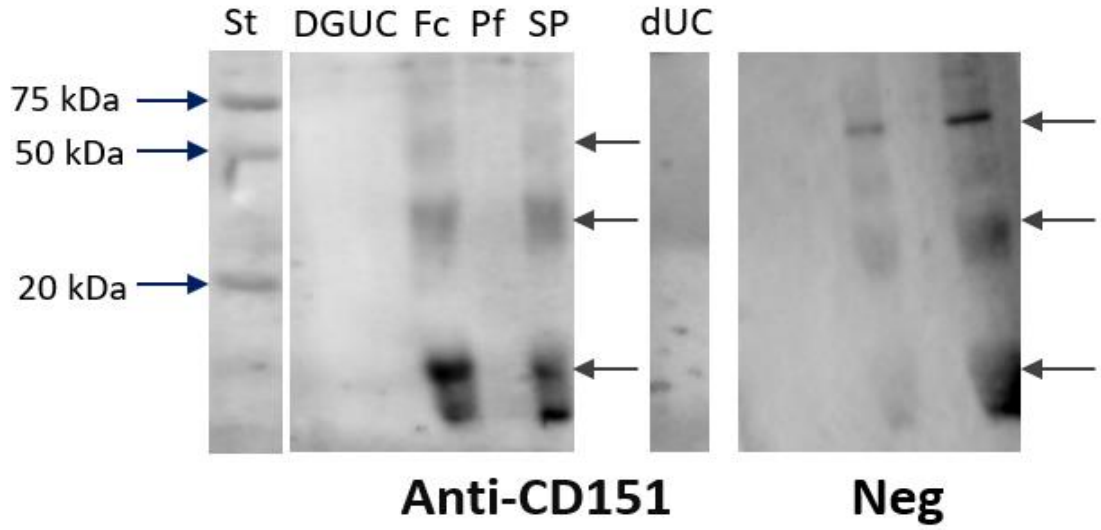
St
DGUC
Fc
Pf
SP
dUC
75 kDa
50 kDa
20 kDa
Anti-CD151
Neg

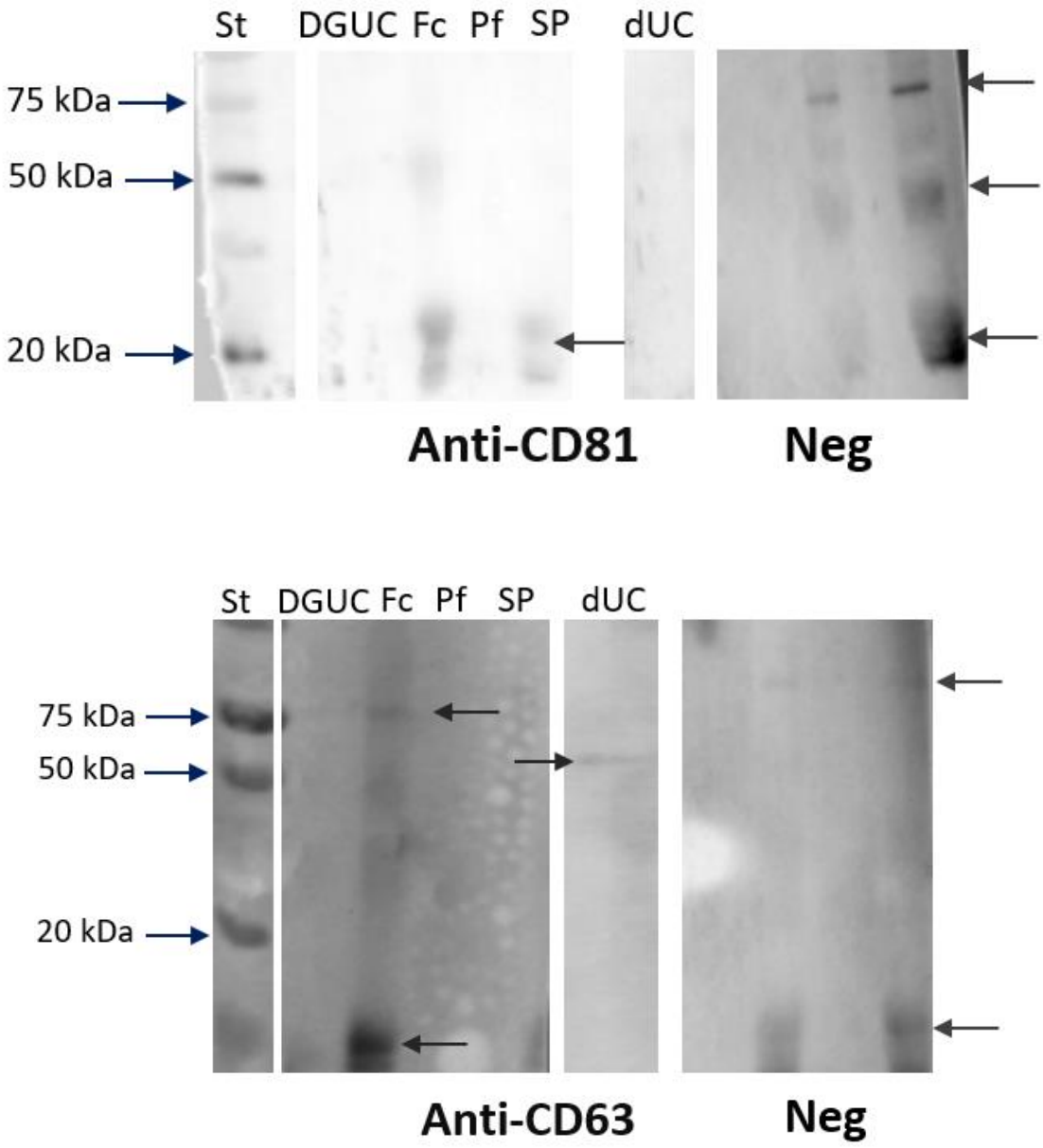

Figure 15: Immunodetection of CD9, CD151, CD81 and CD63 tetraspanins comparing ultracentrifugation methods with protein isolation in reducing basic conditions. St – molecular standard, DGUC – density gradient ultracentrifugation, Fc – filtration from purified SP with collected exosomes, Pf – post-filtration residue, SP – purified seminal plasma. dUC – differential ultracentrifugation. Neg – negative controls with anti-rabbit (for CD9, CD151 and CD81 detection) and anti-mouse (for CD63 detection) secondary antibodies. Grey arrows show non-specific bands.

Subsequently, the EVs' samples obtained through dUC fractionation were subjected to an acidic protocol for protein isolation using a reducing RIPA buffer. This approach yielded more promising outcomes, as bands within the 25 and 29-31 kDa range of CD9, CD151, and CD81, respectively, were evident on the western blot membranes (see **Fig. 16**).

Bands specific for CD63 were not detectable. Although the intensity of the observed bands in a 20-50 kDa region was rather low and further experiments should be conducted to confirm the presence of tetraspanins or to determine the reason for the low intensity of the observed bands. In addition, the strong bands around 75 kDa (grey arrows) were observed with CD9, CD151 and CD81 antibodies.

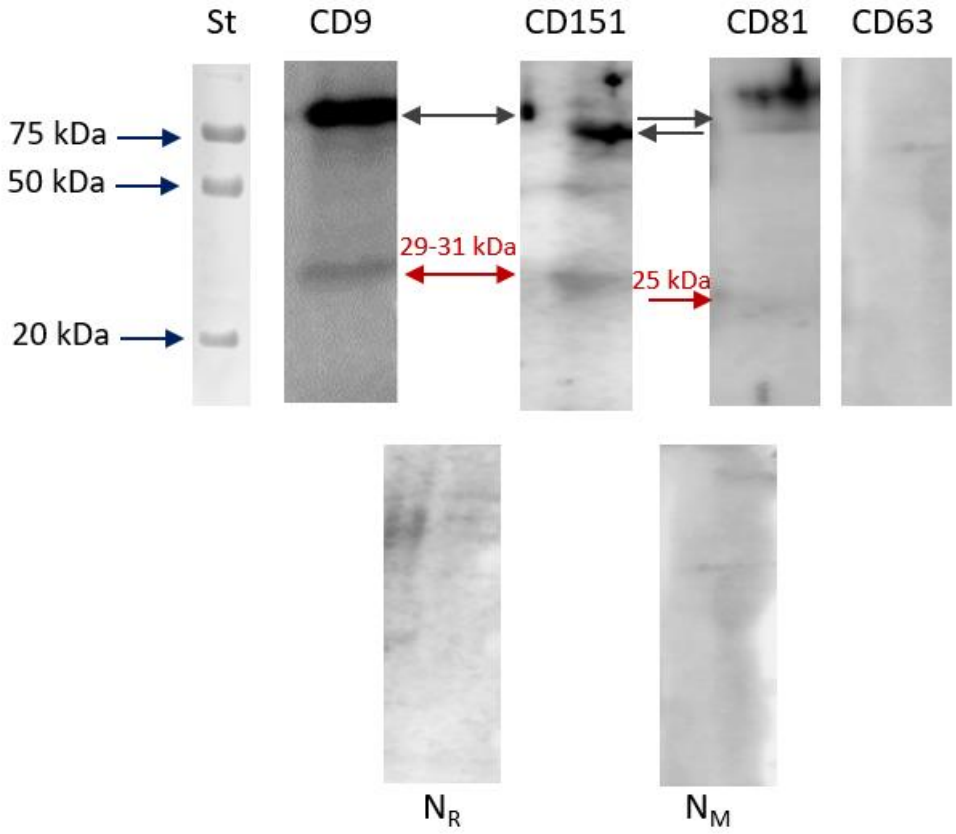

Figure 16: Immunodetection of CD9, CD151, CD81 and CD63 tetraspanins in EVs isolated from boar seminal plasma using differential ultracentrifugation (dUC) method with protein isolation in reducing acidic conditions. St – molecular standard, NR – negative control with anti-rabbit (CD9, CD151, CD81) secondary antibody, NM – negative control with anti-mouse (CD63) secondary antibody. Non-specific bands are indicated with grey arrows, specific bands with red arrows.

Samples obtained under dUC, acidic (Ac) and basic (Bs) reducing buffer conditions were used for integrin alpha V and spermadhesins' (AWN, AQN, PSP1) detection. As for integrin alpha V, two bands around 128-130 kDa were detectable on the membrane in EVs' samples prepared under both acidic and basic conditions, with slightly more intense bands for basic conditions (see **Fig. 17**). There were also observed, specific bands in the range 12-17 and 11-15 kDa for the AQN, AWN and PSP1 proteins, respectively, for both acidic (Ac) and basic (Bs) conditions (see **Fig. 18**). The membranes with negative controls for all protein detections showed no positive reaction.

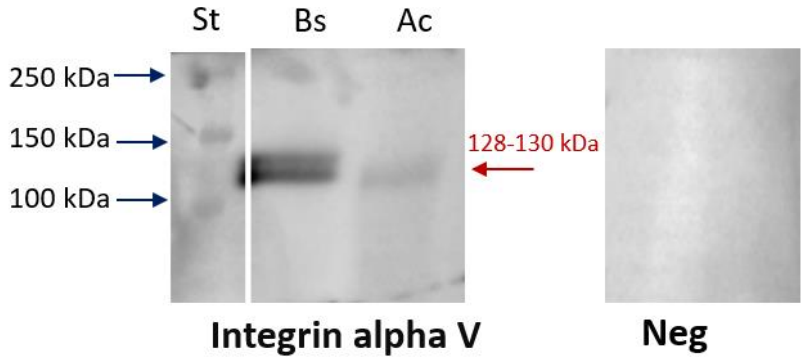

Figure 17: Immunodetection of integrin alpha V in isolated EVs from boar seminal plasma. St – molecular standard, Bs – basic conditions, Ac – acidic conditions, Neg – negative control. Bands are indicated with red arrow.

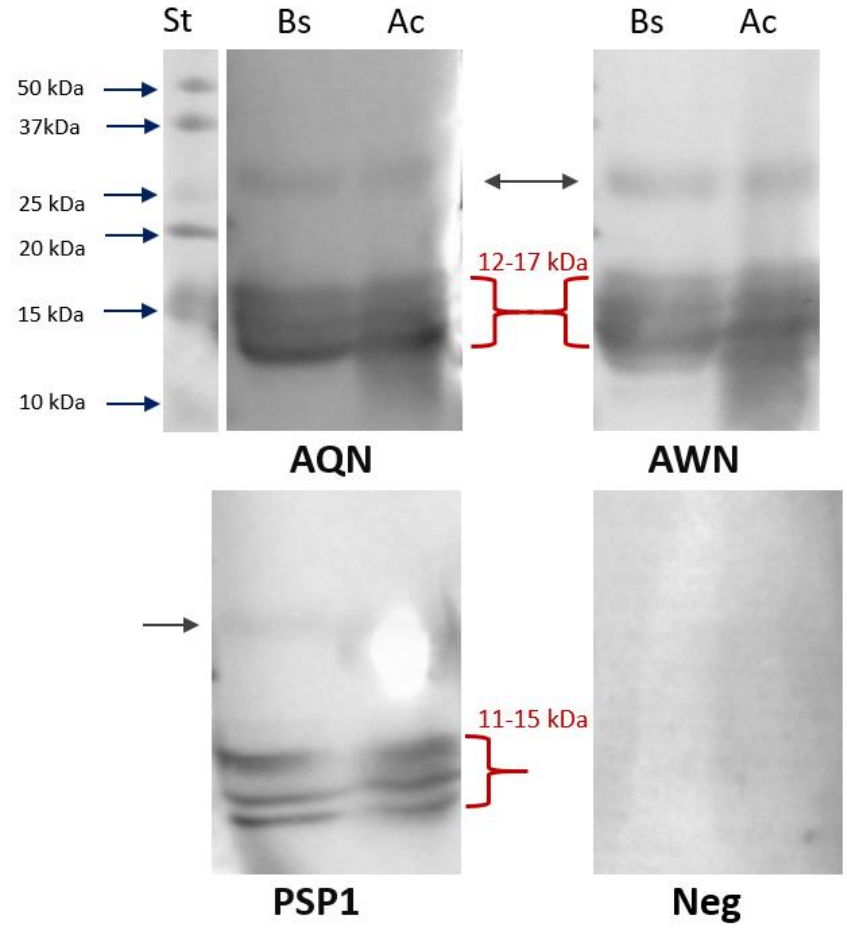

Figure 18: Immunodetection of spermadhesins (AQN, AWN, PSP1) in isolated EVs from boar seminal plasma. St – molecular standard, Bs – basic conditions, Ac – acidic conditions, Neg – negative control. Bands are indicated with red brackets. Non-specific bands are denoted with grey arrows.

5.2 Discussion

The presence of EVs in all biological fluids (Yanez-Mo et al. 2015) indicates their important role in normal body functionality. Human SP was one of the first reproductive fluids in which EVs were confirmed (Ronquist et al. 1978). For the last decade, several studies have reported the presence of EVs in SP of other species such as bull (Alves et al. 2021), stallion (Arienti et al. 1998; Twenter et al. 2020), ram (Leahy et al. 2020) and boar (Du et al. 2016; Barranco et al. 2019; Xu et al. 2020). By delivering an important cargo – proteins, nucleic acids, and lipids – these small nanostructures work as effective cell transporters. The most popular biomarkers used for EVs identification are CD9, CD81, CD151, and CD63 proteins (Barranco et al. 2019; Brzozowski et al. 2018). They are members of large tetraspanin superfamily proteins, which are highly abundant in EVs, especially in exosomes (Jankovicova et al. 2020c). However, only two studies from Barranco et al. (2019) and Du et al. (2016) confirmed the presence of CD9, CD81, and CD63 proteins from isolated boar sEVs. Furthermore, according to Du et al. (2016) the AWN, a member of the spermadhesin family, was also present in isolated porcine sEVs.

In this study, we have focused on the isolation, detection and protein profiling of boar sEVs. The first step was a sequence of consequent centrifugations that allowed us to purify SP from spermatozoa and bigger cell debris. To isolate EVs and remove other smaller membrane particles, the «gold standard» – ultracentrifugation – was chosen as the main technique. To start with, we chose a DGUC protocol using sucrose to create a density gradient and PBS as a buffer. According to Zhang et al. (2014), the DGUC is more comprehensive and more efficient, than other methods. DGUC is considered to be a time-consuming and hard-to-prepare method. Nevertheless, it was chosen to facilitate better separation and, thus, better results. Unfortunately, this separation technique provided us with no results. The SDS gel electrophoresis and Coomassie gel staining of acquired EVs fraction (see **Fig. 14A**) showed no protein present in samples containing estimated EVs. In addition to the DGUC sample, the lane loaded with SP filtered through the membrane filter (**Fc**) is also shown in **Fig. 14A**. As seen from the Fc results, a high protein concentration provides us with no specific readout. The filtration approach proved to be unpromising for sEVs isolation. We assume that the reason for unsuccessful DGUC isolation could be a tendency for EVs to form a specific gel-like structure under ultracentrifugation conditions. When we placed the samples on the gradient and subjected them to centrifugation, we could not separate the vesicles and proteins of different sizes from each other. Everything was agglomerated together in an amorphous gel-like structure. That is why we replaced PBS with saline solution because saline showed to be better in dissolving these structures. Apart from replacing buffers, we have also changed the DGUC to the dUC method, ultracentrifugation without gradient. Based on the electrophoresis and gel staining, this approach provided positive results on protein presence (see **Fig. 14B**). But the presence of proteins itself does not mean successful EVs' isolation. Those proteins could have possibly come from other components of SP.

With positive results in hand, further identification methods were applied. Based on research by Zhang et al. (2014), Barranco et al. (2019) and Du et al. (2016), we decided to

confirm the presence of EVs by TEM using negative staining as a sample preparation method. We resuspended the gel-like pellets in two different buffer types – HEPES and saline buffer. Both buffers contained trehalose dihydrate in a 25 mM concentration. We used this disaccharide membrane protectant to prevent EVs' aggregation. Finally, results from TEM showed the presence of vesicles about 20-500 nm in size (see **Fig. 7-8**), which correspond not only to exosomes but also to MVs. Although both buffers provided comparable results, the saline buffer showed worse results due to the high salt amount, which could be observed in the background (see **Fig. 8**). For the negative staining method used for TEM sample preparation, a saline buffer was generally sufficient, despite a tendency for salt crystallization. In case one wants to further investigate the identification of proteins situated on vesicles, another visualization technique, such as cryo-EM, should be considered. In this context, the use of HEPES buffer would be a better choice than the saline buffer.

By MS analysis we investigated the exact protein composition of the isolated EVs. The MS analysis (see **Fig. 9-12**; **Tab. 1** and **2**) revealed unexpected and controversial results. Firstly, the overall low protein abundance and, secondly, the absence of tetraspanin and integrin family proteins in the analyzed samples. This result was unexpected, as the presence of tetraspanins in boar sEVs was confirmed in recent studies by Barranco et al. (2019) using nanoscale flow cytometry and by Du et al. (2016) using Western blot analysis. In contrast to the results discussed above, a higher number of spermadhesins were found instead. Since spermadhesins are secretory proteins derived from reproductive tissues, it is possible that these proteins may be attached to the EVs' PM surface or be inside it (van Tilburg et al. 2021). It is also possible for soluble SP protein contamination to be present. However, based on Western blot results with AWN and PSP1 spermadhesins detection in boar sEVs by Du et al. (2016), we assume that boar sEVs could contain spermadhesins.

There could be several reasons for low protein identification rates during MS analysis. Firstly, the number of peptides used for the analysis may be insufficient for the detection limit of the MS instrument. As a possible solution, the engagement of affinity-based enrichment protocols in combination with MS analysis may help to enlarge the protein amount sufficient for MS detection limits. Secondly, tetraspanins are known to be incorporated into the membrane bilayer, with only a small amino acid tail visible from the outer membrane layer. The reason for the low protein amount could be an inappropriate peptide isolation protocol – it is possible that proteins of interest were not extracted under the provided conditions. On the other hand, the isolation conditions might not allow proper solubilization of proteins incorporated inside a membrane. To overcome such problems, different detergents and buffer combinations can be tested for solubilization of the lipid membrane and extraction of the incorporated tetraspanins.

For successful protein identification, proteins have to be digested into peptides before being analyzed by MS. Each peptide is then identified based on its charge-to-mass ratio and specific fragmentation patterns. Unfortunately, the search for peptides can be complicated by the presence of post-translational modifications (PTMs) on them. Although it is possible to perform a search for proteins taking into account different PTMs, one should provide information about the exact amino acid where PTM may occur, the exact mass shift caused by this PTM and the possible amount of such PTMs. An example of PTM that may take

place in tetraspanins is glycosylation – the addition of carbohydrate molecules, such as monosaccharides or polysaccharides. As we cannot provide specific information about the modification, it is possible that we did not detect tetraspanins and integrins due to PTMs occurring on this protein.

Inspired by the method of Al-Dossary et al. (2013), we co-incubated isolated and membrane-stained EVs with boar spermatozoa and successfully observed the sperm-EVs interaction. The most intense signals were observed on the PM in the acrosomal and tail regions of the spermatozoa. The vesicles observed in these regions tended to be larger in volume, or they may have formed agglomerations. It is worth mentioning that during the co-incubation, the vesicles specifically interacted with the PM without penetrating it.

It is also worth mentioning, that for this experiment we used an ejaculated spermatozoa for simplicity, but the better option would be to use spermatozoa from cauda epididymis. In this case, sperm may interact naturally with SP. In addition, the isolation of OVS and their cargo to ejaculated spermatozoa could possibly bring even more benefits to understanding their mutual interaction, affecting sperm fertility and mechanisms of such processes as capacitation and spermatozoa maturation (Al-Dossary et al. 2013; Bathala et al. 2018).

Our next goal was EVs detection using specific exosomal markers. According to Barranco et al. (2019) study, the above-mentioned tetraspanins (CD9, CD81, CD63) were used as prior markers for EVs detection. We were also interested in CD151 tetraspanin, which presence was already confirmed in human prostasomes (Brzozowski et al.2018), women triple-negative breast cancer (TNBC) exosomes (Li et al. 2021), mice epididymosomes (Nixon et al. 2019) and human, mice, bull (Jankovicova et al. 2020a), and boar (Dobrodinska 2020) spermatozoa. But nobody has not been tried yet to detect in boar EVs. Based on the results of MS analysis from Du et al. (2016), we also used specific antibodies for the detection of the spermadhesins (AWN, PSP1, AQN). Furthermore, following the results of Al-Dossary et al. (2013) on integrin involvement in mouse OVS-sperm interaction, we added an antibody against integrin alpha V to our experiments to detect the presence of this protein on boar sEVs. It was also important to successfully extract proteins from isolated sEVs after ultracentrifugation for further immunodetection.

From the beginning, we used basic conditions to dissolve the EVs pellet fraction. We applied this protein isolation method under basic conditions (Pendergrast et al. 2020) to both ultracentrifugation techniques. Tetraspanins are tend to form a tetraspanin web containing a specific set of proteins (van Deventer et al. 2017). Unfortunately, even after successful dUC and detection of protein bands in Coomassie-stained gel, the immunodetection and MS analysis for tetraspanins in basic conditions showed no results (see **Fig. 15**). According to these results, we can assume that the extraction of proteins based on the basic conditions is an unsuitable method for tetraspanins. In addition, there are currently no antibodies on the market specifically to these porcine proteins, which makes their detection even more difficult.

Next, we modified the protocol and changed basic conditions for acidic conditions (Brennan et al. 2020) during protein isolation. The immunodetection results on CD9, CD151 and CD81 showed bands with molecular weight in a range of 25-31 kDa (see **Fig. 16**), that correlate with tetraspanin molecular weight. However, those bands had weak intensity, and

their presence was not constant for each immunodetection. We were not able to confirm a successful detection of these proteins in boar sEVs. Additionally, with similar results from Kupcova Skalnikova et al. (2019), we did not find any positive signal for CD63 during our study. Also, we can spot high-intensity bands in the region of 70 kDa (see **Fig. 16**, grey arrows). This observation corresponds with the fact that different isoforms of tetraspanins can either be predominantly as a monomer or create dimers with other tetraspanins through disulfide bonds. This observation suggests that the reduction efficiency may be insufficient, resulting in proteins remaining in the dimer form with or without PTMs (Frolikova et al 2018). Another reason for unsuccessful immunodetection could be an inappropriate sample preparation causing either a change of the structure or even the destruction of the protein epitope itself. This is our second assumption why antibodies could not recognize the proteins of interest. We hope, that with the advent of suitable antibodies and appropriate isolation protocol, future studies will be more successful in this field.

On the other hand, we were able to detect the highly intense band of integrin alpha V (see **Fig. 17**) and all three spermadhesin proteins (see **Fig. 18**). Spermadhesins detection corresponds with study results from Du et al. (2016) and finding AWN and PSP1 proteins. As mentioned before, we also found all three types of spermadhesins using MS analysis (see **Fig. 10**, **Tab. 1** and **2**), so for future studies will be important to confirm that they are part of sEVs by immunodetection directly on the vesicles using TEM. Integrin alpha V was identified in mouse, porcine and human sperm (Palenikova et al. 2021). Furthermore, the facilitation of integrins in the fusion of OVS in the delivery of transmembrane proteins to mouse spermatozoa has already been confirmed by Al-Dossary et al. (2013). The involvement of this protein in reproductive processes is already beyond doubt, but it will be interesting to verify whether this protein gets from the EVs to the spermatozoa.

In summary, while our study faced challenges in isolating EVs from boar SP, we were able to achieve positive results using dUC. We confirmed the presence of EVs through TEM and identified specific proteins using MS. This study contributes to the growing body of research on EVs in reproductive fluids and highlights the potential importance of OVS in sperm and oocyte maturation, sperm capacitation and even embryo development. It suggests new goals to solve to find promising applications in the field of biotechnology.

6 Conclusion

The primary objective of this diploma thesis was to investigate the promising field of protein composition in EVs isolated from the boar seminal plasma. Current knowledge in this area is limited, with few publications describing robust isolation techniques and little information available on EVs' composition. In this study, we tested three isolation techniques, including filtration, DGUC, and dUC. Filtration did not provide promising results and was rejected, while the DGUC approach yielded inconsistent results and was technically challenging and time-consuming. Only using the dUC technique we were able to successfully isolate vesicle-like structures with characteristic shapes and sizes that were later confirmed by electron microscopy.

Mass spectrometry analysis of isolated vesicles revealed the presence of spermadhesins, which was further confirmed by western blot analysis. We also confirmed the presence of integrin alpha V, but this result was not supported by MS. The study also investigated the presence of tetraspanins, which are considered to be primary biomarkers of EVs. Sample preparation for immunolabelling techniques such as Western blot to detect tetraspanins can be challenging. Degradation of tetraspanins epitopes in the outer layer of the membrane caused by harsh isolation conditions can be a major problem for identification, which we encountered in this study.

In addition, the presence of tetraspanins in the boar seminal plasma has not been confirmed by MS probably due to their hydrophobic nature and tendency to be incorporated into the cell membrane. Special sample preparation for MS measurement is required to improve tetraspanin identification.

Although the evidence for other EVs' biomarkers, such as tetraspanins, was inconclusive, the results of this study have laid the groundwork for further research into EVs in the mammalian reproductive system. Future studies can build on these findings by further exploring EVs' isolation techniques and investigating the potential role of EVs and their biomarkers in reproductive biology.

7 References

Abels ER, Breakefield XO. 2016. Introduction to extracellular vesicles: biogenesis, RNA cargo selection, content, release, and uptake. Cellular and molecular neurobiology **36**: 301-312.

Al-Dossary AA, Strehler EE, Martin-DeLeon PA. 2013. Expression and secretion of plasma membrane Ca2+-ATPase 4a (PMCA4a) during murine estrus: association with oviductal exosomes and uptake in sperm. PloS one **8**(11): e80181.

Almiñana C, Corbin E, Tsikis G, Alcântara-Neto AS, Labas V, Reynaud K, Galio L, Uzbekov R, Garanina AS, Druart X, Mermillod P. 2017. Oviduct extracellular vesicles protein content and their role during oviduct–embryo cross-talk. Reproduction **154**(3): 253-268.

Alvarez-Rodriguez M, Ljunggren SA, Karlsson H, Rodriguez-Martinez H. 2019. Exosomes in specific fractions of the boar ejaculate contain CD44: A marker for epididymosomes? Theriogenology **140**: 143-152.

Alves MBR, de Arruda RP, Batissaco L, Garcia-Oliveros LN, Gonzaga VHG, Nogueira VJM, dos Santos Almeida F, Pinto SCC, Andrade GM, Perecin F, da Silveira JC, Celeghini ECC. 2021. Changes in miRNA levels of sperm and small extracellular vesicles of seminal plasma are associated with transient scrotal heat stress in bulls. Theriogenology **161**: 26-40.

Andreu Z, Yáñez-Mó M. 2014. Tetraspanins in extracellular vesicle formation and function. Frontiers in immunology **5**: 442.

Antalíková J, Jankovičová J, Simon M, Cupperová P, Michalková K, Horovská Ľ. 2015. Localization of CD 9 molecule on bull spermatozoa: its involvement in the sperm–egg interaction. Reproduction in domestic animals **50**(3): 423-430.

Arienti G, Carlini E, De Cosmo AM, Di Profio P, Palmerini CA. 1998. Prostasome-like particles in stallion semen. Biology of reproduction **59**(2): 309-313.

Babst M. 2011. MVB vesicle formation: ESCRT-dependent, ESCRT-independent and everything in between. Current opinion in cell biology **23**(4): 452-457.

Barranco I, Padilla L, Parrilla I, Álvarez-Barrientos A, Pérez-Patiño C, Peña FJ, Martínez EA, Rodriguez-Martínez H, Roca J. 2019. Extracellular vesicles isolated from porcine seminal plasma exhibit different tetraspanin expression profiles. Scientific reports **9**(1): 11584.

Bassani S, Cingolani LA. 2012. Tetraspanins: Interactions and interplay with integrins. The international journal of biochemistry & cell biology **44**(5): 703-708.

Bathala P, Fereshteh Z, Li K, Al-Dossary AA, Galileo DS, Martin-DeLeon PA. 2018. Oviductal extracellular vesicles (oviductosomes, OVS) are conserved in humans: murine OVS play a pivotal role in sperm capacitation and fertility. MHR: Basic science of reproductive medicine **24**(3): 143-157.

Battistelli M, Falcieri E. 2020. Apoptotic bodies: Particular extracellular vesicles involved in intercellular communication. Biology **9**(1): 21.

Berditchevski F, Odintsova E. 2007. Tetraspanins as regulators of protein trafficking. Traffic **8**(2): 89-96.

Bidarimath M. Khalaj K, Kridli RT, Kan FW, Koti M, Tayade C. 2017. Extracellular vesicle mediated intercellular communication at the porcine maternal-fetal interface: A new paradigm for conceptus-endometrial cross-talk. Scientific reports **7**(1): 1-14.

Boucheix C, Rubinstein E. 2001. Tetraspanins. Cellular and Molecular Life Sciences CMLS **58**: 1189-1205.

Brennan K, Martin K, FitzGerald, SP, O'sullivan J, Wu Y, Blanco A, Mc Gee MM. 2020. A comparison of methods for the isolation and separation of extracellular vesicles from protein and lipid particles in human serum. Scientific reports. **10**(1): 1039.

Brzozowski JS, Bond DR, Jankowski H, Goldie BJ, Burchell R, Naudin C, Smith ND, Scarlett CJ, Larsen MR, Dun MD, Skelding KA, Weidenhofer J. 2018. Extracellular vesicles with altered tetraspanin CD9 and CD151 levels confer increased prostate cell motility and invasion. Scientific reports **8**(1): 1-13.

Burkova EE, Dmitrenok PS, Bulgakov DV, Vlassov VV, Ryabchikova EI, Nevinsky GA. 2018. Exosomes from human placenta purified by affinity chromatography on sepharose bearing immobilized antibodies against CD81 tetraspanin contain many peptides and small proteins. IUBMB life **70**(11): 1144-1155.

Burns G, Brooks K, Wildung M, Navakanitworakul R, Christenson LK, Spencer TE. 2014. Extracellular vesicles in luminal fluid of the ovine uterus. PloS one **9**(3): e90913.

Caballero JN, Frenette G, Belleannée C, Sullivan R. 2013. CD9-positive microvesicles mediate the transfer of molecules to bovine spermatozoa during epididymal maturation. PloS one **8**(6): e65364.

Carroll-Portillo A, Surviladze Z, Cambi A, Lidke DS, Wilson BS. 2012. Mast cell synapses and exosomes: membrane contacts for information exchange. Frontiers in immunology **3**: 46.

Chairoungdua A, Smith DL, Pochard P, Hull M, Caplan MJ. 2010. Exosome release of β-catenin: a novel mechanism that antagonizes Wnt signaling. Journal of Cell Biology **190**(6): 1079-1091.

Chargaff E, West R. 1946. The biological significance of the thromboplastic protein of Wood. Journal of Biological Chemistry **166**: 189-197.

Charrin S, Jouannet S, Boucheix C, Rubinstein E. 2014. Tetraspanins at a glance. Journal of cell science **127**(17): 3641-3648.

Claas C, Stipp CS, Hemler ME. 2001. Evaluation of prototype transmembrane 4 superfamily protein complexes and their relation to lipid rafts. Journal of Biological Chemistry **276**(11): 7974-7984.

Colombo M, Raposo G, Théry C. 2014. Biogenesis, secretion, and intercellular interactions of exosomes and other extracellular vesicles. Annual review of cell and developmental biology **30**: 255-289.

Crescitelli R, Lässer C, Szabo TG, Kittel A, Eldh M, Dianzani I, Buzás EI, Lötvall J. 2013. Distinct RNA profiles in subpopulations of extracellular vesicles: apoptotic bodies, microvesicles and exosomes. Journal of extracellular vesicles **2**(1): 20677.

Cupperová P, Simon M, Antalíková J, Michalková K, Horovská Ľ, Hluchý S. 2014. Distribution of tetraspanin family protein CD9 in bull reproductive system. Czech Journal of Animal Science **59**(3): 134-139.

Cvjetkovic A, Lötvall J, Lässer C. 2014. The influence of rotor type and centrifugation time on the yield and purity of extracellular vesicles. Journal of extracellular vesicles **3**(1): 23111.

Da Silveira JC, Andrade GM, Del Collado M, Sampaio RV, Sangalli JR, Silva LA, Pinaffi FVL, Jardim IB, Cesar MC, Nogueira MFG, Cesar ASM, Coutinho LL, Pereira RW, Perecin F, Meirelles FV. 2017. Supplementation with small-extracellular vesicles from ovarian follicular fluid during in vitro production modulates bovine embryo development. PloS one **12**(6): e0179451.

Da Silveira JC, Veeramachaneni DR, Winger QA, Carnevale EM, Bouma GJ. 2012. Cell-secreted vesicles in equine ovarian follicular fluid contain miRNAs and proteins: a possible new form of cell communication within the ovarian follicle. Biology of reproduction **86**(3): 71-1.

Dalton AJ. 1975. Microvesicles and vesicles of multivesicular bodies versus "virus-like" particles. Journal of the National Cancer Institute **54**(5): 1137-1148.

Dobrodinská A. 2020. Detekce tetraspaninů v samčím reprodukčním traktu a spermiích. [MSc. Thesis]. Czech University of Life Sciences Prague, Prague.

Doyle LM, Wang MZ. 2019. Overview of extracellular vesicles, their origin, composition, purpose, and methods for exosome isolation and analysis. Cells **8**(7): 727.

Du J, Shen J, Wang Y, Pan C, Pang W, Diao H, Dong W. 2016. Boar seminal plasma exosomes maintain sperm function by infiltrating into the sperm membrane. Oncotarget **7**(37): 58832.

Elzanowska J, Semira C, Costa-Silva B. 2021. DNA in extracellular vesicles: Biological and clinical aspects. Molecular Oncology **15**(6): 1701-1714.

Escola JM, Kleijmeer MJ, Stoorvogel W, Griffith JM, Yoshie O, Geuze HJ. 1998. Selective enrichment of tetraspanin proteins on the internal vesicles of multivesicular endosomes and on exosomes secreted by human B-lymphocytes. Journal of Biological Chemistry **273**(32): 20121-20127.

Fereshteh Z, Schmidt SA, Al-Dossary AA, Accerbi M, Arighi C, Cowart J, Song JL, Green PJ, Choi K, Yoo S, Martin-DeLeon PA. 2018. Murine Oviductosomes (OVS) microRNA profiling during the estrous cycle: Delivery of OVS-borne microRNAs to sperm where miR-34c-5p localizes at the centrosome. Scientific Reports **8**(1): 16094.

Fischer von Mollard G, Mignery GA, Baumert M, Perin MS, Hanson TJ, Burger PM, Jahn R, Südhof TC. 1990. rab3 is a small GTP-binding protein exclusively localized to synaptic vesicles. Proceedings of the National Academy of Sciences **87**(5): 1988-1992.

Fornés MW, De Rosas JC. 1991. Interactions between rat epididymal epithelium and spermatozoa. The Anatomical Record **231**(2): 193-200.

Frenette G, Sullivan R. 2001. Prostasome-like particles are involved in the transfer of P25b from the bovine epididymal fluid to the sperm surface. Molecular Reproduction and Development: Incorporating Gamete Research **59**(1): 115-121.

Frolíková M, Manaskova-Postlerová P, Cerný J, Jankovičová J, Šimoník O, Pohlova A, Sečová P, Antalíková J, Dvorakova-Hortova K. 2018. CD9 and CD81 interactions and their structural modelling in sperm prior to fertilization. International journal of molecular sciences **19**(4): 1236.

Gatti JL, Métayer S, Moudjou M, Andréoletti O, Lantier F, Dacheux JL, Sarradin P. 2002. Prion protein is secreted in soluble forms in the epididymal fluid and proteolytically processed and transported in seminal plasma. Biology of reproduction **67**(2): 393-400.

Gervasi MG, Visconti PE. 2017. Molecular changes and signaling events occurring in spermatozoa during epididymal maturation. Andrology **5**(2): 204-218.

Ghossoub R, Lembo F, Rubio A, Gaillard CB, Bouchet J, Vitale N, Slavík J, Machala M, Zimmermann P. 2014. Syntenin-ALIX exosome biogenesis and budding into multivesicular bodies are controlled by ARF6 and PLD2. Nature communications **5**(1): 3477.

Giacomini E, Vago R, Sanchez AM, Podini P, Zarovni N, Murdica V, Rizzo R, Bortolotti D, Candiani M, Viganò P. 2017. Secretome of in vitro cultured human embryos contains extracellular vesicles that are uptaken by the maternal side. Scientific Reports **7**(1): 5210.

Girouard J, Frenette G, Sullivan R. 2011. Comparative proteome and lipid profiles of bovine epididymosomes collected in the intraluminal compartment of the caput and cauda epididymis. International journal of andrology **34**(5pt2): e475-e486.

Grdisa M, Mathew A, and Johnstone RM. 1993. Expression and loss of the transferrin receptor in growing and differentiating HD3 cells. Journal of cellular physiology **155** (2): 349-357.

Hanson PI, Cashikar A. 2012. Multivesicular body morphogenesis. Annual review of cell and developmental biology **28**: 337-362.

Heijnen HF, Schiel AE, Fijnheer R, Geuze HJ, Sixma JJ. 1999. Activated Platelets Release Two Types of Membrane Vesicles: Microvesicles by Surface Shedding and Exosomes Derived From Exocytosis of Multivesicular Bodies and α-Granules. Blood, The Journal of the American Society of Hematology **94**(11): 3791-3799.

Hemler ME. 2005. Tetraspanin functions and associated microdomains. Nature reviews Molecular cell biology **6**(10): 801-811.

Hessvik NP, Llorente A. 2018. Current knowledge on exosome biogenesis and release. Cellular and Molecular Life Sciences **75**: 193-208.

Huang A, Isobe N, Yoshimura Y. 2017. Changes in localization and density of CD63-positive exosome-like substances in the hen oviduct with artificial insemination and their effect on sperm viability. Theriogenology **101**: 135-143.

Huang S, Yuan S, Dong M. 2005. The phylogenetic analysis of tetraspanins projects the evolution of cell–cell interactions from unicellular to multicellular organisms. Genomics **86**(6): 674-684.

Huang X, Yuan T, Tschannen M, Sun Z, Jacob H, Du M, Liang M, Dittmar RL, Liu Y, Liang M, Kohli M, Thibodeau SN, Boardman L, Wang L. 2013. Characterization of human plasma-derived exosomal RNAs by deep sequencing. BMC genomics **14**(1): 1-14.

Hung WT, Hong X, Christenson LK, McGinnis LK. 2015. Extracellular vesicles from bovine follicular fluid support cumulus expansion. Biology of reproduction **93**(5): 117-1.

Jankovičová J, Frolíková M, Palenikova V, Valašková E, Černý J, Sečová P, Bartoková M, Horovska L, Maňáskova-Postlerová P, Antalíková J, Komrsková K. 2020.

Expression and distribution of CD151 as a partner of alpha6 integrin in male germ cells. Scientific Reports **10**(1): 1-12. A

Jankovičová J, Frolíková M, Šebková N, Simon M, Cupperová P, Lipcseyova D, Katarina Michalková K, Horovská L, Sedlaček R, Stopka P, Antalíková J, Dvorakova-Hortova K. 2016. Characterization of tetraspanin protein CD81 in mouse spermatozoa and bovine gametes. Reproduction **152**(6): 785-793.

Jankovičová J, Neuerová Z, Sečová P. 2020. Tetraspanins in mammalian reproduction: spermatozoa, oocytes and embryos. Medical microbiology and immunology **209**: 407-425. B

Jankovičová J, Sečová P, Maňáskova-Postlerová P, Šimoník O, Frolíková M, Chmelíková E, Horovská L, Michalková K, Dvorakova-Hortova K, Antalíková J. 2019. Detection of CD9 and CD81 tetraspanins in bovine and porcine oocytes and embryos. International journal of biological macromolecules **123**: 931-938.

Jankovičová J, Sečová P, Michalková K, Antalíková J. 2020. Tetraspanins, More than Markers of Extracellular Vesicles in Reproduction. International Journal of Molecular Sciences 21(20), 30: 7568. C

Jankovičová J, Simon M, Antalíková J, Cupperová, P, Michalková K. 2015. Role of tetraspanin CD9 molecule in fertilization of mammals. Physiological research **64**(3): 279-293

Johnstone RM, Adam M, Hammond JR, Orr L, Turbide C. 1987. Vesicle formation during reticulocyte maturation. Association of plasma membrane activities with released vesicles (exosomes). Journal of Biological Chemistry **262**(19): 9412-9420.

Johnstone RM, Mathew A, Mason AB, Teng K. 1991. Exosome formation during maturation of mammalian and avian reticulocytes: evidence that exosome release is a major route for externalization of obsolete membrane proteins. Journal of cellular physiology **147**(1): 27-36.

Juyena NS, Stelletta C. 2013. Seminal plasma: an essential attribute to spermatozoa. Journal of andrology **33**(4): 536-551.

Kaewmala K, Uddin MJ, Cinar MU, Große-Brinkhaus C, Jonas E, Tesfaye D, Phatsara C, Tholen E, Looft C, Schellander K. 2011. Association study and expression analysis of CD9 as candidate gene for boar sperm quality and fertility traits. Animal reproduction science **125**(1-4): 170-179.

Kaji K, Oda S, Shikano T. 2000. The gamete fusion process is defective in eggs of Cd9-deficient mice. Nature genetics **24**(3): 279-282.

Kalra H, Drummen GP, Mathivanan S. 2016. Focus on extracellular vesicles: introducing the next small big thing. International journal of molecular sciences 17(2): 170.

Kanatsu-Shinohara M, Toyokuni S, Shinohara T. 2004. CD9 is a surface marker on mouse and rat male germline stem cells. Biology of reproduction **70**(1): 70-75.

Kim KM, Abdelmohsen K, Mustapic M, Kapogiannis D, Gorospe M. 2017. RNA in extracellular vesicles. Wiley Interdisciplinary Reviews: RNA **8**(4): e1413.

Kshirsagar SK, Alam SM, Jasti S, Hodes H, Nauser T, Gilliam M, Billstrand C, Hunt JS, Petroff, MG. 2012. Immunomodulatory molecules are released from the first trimester and term placenta via exosomes. Placenta **33**(12): 982-990.

Kupcova Skalnikova H, Bohuslavova B, Turnovcova K, Juhasova J, Juhas S, Rodinova M, Vodicka P. 2019. Isolation and characterization of small extracellular vesicles from porcine blood plasma, cerebrospinal fluid, and seminal plasma. Proteomes **7**(2): 17.

Lang T, Hochheimer N. 2020. Tetraspanins. Current Biology **30**(5): R204-R206.

Lange-Consiglio A, Perrini C, Albini G, Modina S, Lodde V, Orsini E, Cremonesi F. 2017. Oviductal microvesicles and their effect on in vitro maturation of canine oocytes. Reproduction **154**(2): 167-180.

Latysheva N, Muratov G, Rajesh S, Padgett M, Hotchin NA, Overduin M, Berditchevski F. 2006. Syntenin-1 is a new component of tetraspanin-enriched microdomains: mechanisms and consequences of the interaction of syntenin-1 with CD63. Molecular and Cellular Biology **26**(20): 7707-7718.

Laulagnier K, Motta C, Hamdi S, Roy S, Fauvelle F, Pageaux JF, Kobayashi T, Salles JP, Perret B, Bonnerot C, Record M. 2004. Mast cell-and dendritic cell-derived exosomes display a specific lipid composition and an unusual membrane organization. Biochemical Journal **380**(1): 161-171.

Lázaro-Ibáñez E, Sanz-Garcia A, Visakorpi T, Escobedo-Lucea C, Siljander P, Ayuso-Sacido Á, Yliperttula M. 2014. Different gDNA content in the subpopulations of prostate cancer extracellular vesicles: apoptotic bodies, microvesicles, and exosomes. The Prostate **74**(14): 1379-1390.

Li P, Kaslan M, Lee SH, Yao J, Gao Z. 2017. Progress in exosome isolation techniques. Theranostics **7**(3): 789.

Li S, Li X, Yang S, Pi H, Li Z, Yao P, Zhang Q, Wang Q, Shen P, Li X, Ji J. 2021. Proteomic landscape of exosomes reveals the functional contributions of CD151 in triple-negative breast cancer. Molecular & cellular proteomics **20**.

Li YH, Hou Y, Ma W, Yuan JX, Zhang D, Sun QY, Wang W H. 2004. Localization of CD9 in pig oocytes and its effects on sperm–egg interaction. Reproduction **127**(2): 151-157.

Livshits MA, Khomyakova E, Evtushenko EG, Lazarev VN, Kulemin NA, Semina SE, Generozov EV, Govorun VM. 2015. Isolation of exosomes by differential centrifugation: Theoretical analysis of a commonly used protocol. Scientific reports **5**(1): 17319.

Llorente A, Skotland T, Sylvänne T, Kauhanen D, Róg T, Orłowski A, Vattulainen I, Ekroos K, Sandvig, K. (2013). Molecular lipidomics of exosomes released by PC-3 prostate cancer cells. Biochimica et Biophysica Acta (BBA)-Molecular and Cell Biology of Lipids **1831**(7): 1302-1309.

Lopera-Vasquez R, Hamdi M, Fernandez-Fuertes B, Maillo V, Beltrán-Breña P, Calle A, Redruello A, López-Martín S, Gutierrez-Adán A, Yañez-Mó M, Ramirez MA, Rizos D. 2016. Extracellular vesicles from BOEC in in vitro embryo development and quality. PloS one **11**(2): e0148083.

Mathivanan S, Ji H, Simpson RJ. 2010. Exosomes: extracellular organelles important in intercellular communication. Journal of proteomics **73**(10):1907-1920.

Mathivanan S, Lim JW, Tauro BJ, Ji H, Moritz RL, Simpson RJ. 2010. Proteomics analysis of A33 immunoaffinity-purified exosomes released from the human colon tumor

cell line LIM1215 reveals a tissue-specific protein signature. Molecular & cellular proteomics **9**(2): 197-208.

Matsuno Y, Kanke T, Maruyama N, Fujii W, Naito K, Sugiura K. 2019. Characterization of mRNA profiles of the exosome-like vesicles in porcine follicular fluid. Plos one **14**(6): e0217760.

Mellisho EA, Velásquez AE, Nuñez MJ, Cabezas JG, Cueto JA, Fader C, Castro FO, Rodríguez-Álvarez L. 2017. Identification and characteristics of extracellular vesicles from bovine blastocysts produced in vitro. PLoS One **12**(5): e0178306.

Miranda KC, Bond DT, McKee M, Skog J, Păunescu TG, Da Silva N, Brown D, Russo LM. 2010. Nucleic acids within urinary exosomes/microvesicles are potential biomarkers for renal disease. Kidney international **78**(2): 191-199.

Miyado K, Yamada G, Yamada S. 2000. Requirement of CD9 on the egg plasma membrane for fertilization. Science **287**(5451): 321-324.

Miyado K, Yoshida K, Yamagata K. 2008. The fusing ability of sperm is bestowed by CD9-containing vesicles released from eggs in mice. Proceedings of the National Academy of Sciences **105**(35): 12921-12926.

Monguió-Tortajada M, Gálvez-Montón C, Bayes-Genis A, Roura S, Borràs FE. 2019. Extracellular vesicle isolation methods: rising impact of size-exclusion chromatography. Cellular and Molecular Life Sciences **76**(12): 2369-2382.

Nabhan JF, Hu R, Oh RS, Cohen SN, Lu Q. 2012. Formation and release of arrestin domain-containing protein 1-mediated microvesicles (ARMMs) at plasma membrane by recruitment of TSG101 protein. Proceedings of the National Academy of Sciences **109**(11): 4146-4151.

Ng YH, Rome S, Jalabert A, Forterre A, Singh H, Hincks CL, Salamonsen LA. 2013. Endometrial exosomes/microvesicles in the uterine microenvironment: a new paradigm for embryo-endometrial cross talk at implantation. PloS one **8**(3): e58502.

Nixon B, De Iuliis GN, Hart HM, Zhou W, Mathe A, Bernstein IR, Anderson AL, Stanger SJ, Skerrett-Byrne DA, Jamaluddin MFB, Almazi JG, Bromfield EG, Larsen MR, Dun MD. (2019). Proteomic profiling of mouse epididymosomes reveals their contributions to post-testicular sperm maturation. Molecular & Cellular Proteomics **18**: S91-S108.

Nolte-'t Hoen EN, Buermans HP, Waasdorp M, Stoorvogel W, Wauben MH, C 't Hoen PA. 2012. Deep sequencing of RNA from immune cell-derived vesicles uncovers the selective incorporation of small non-coding RNA biotypes with potential regulatory functions. Nucleic acids research **40**(18): 9272-9285.

Ohnami N, Nakamura A, Miyado M, Sato M, Kawano M, Yoshida K, Harada Y, Takezawa Y, Kanai S, Ono C, Takahashi Y, Kimura K, Shida T, Miyado K, Umezawa A. 2012. CD81 and CD9 work independently as extracellular components upon fusion of sperm and oocyte. Biology open **1**(7): 640-647.

Palenikova V, Frolikova M, Valaskova E, Postlerova P, Komrskova K. 2021. αV Integrin Expression and Localization in Male Germ Cells. International Journal of Molecular Sciences **22**(17): 9525.

Palmisano G, Jensen SS, Le Bihan MC, Laine J, McGuire JN, Pociot F, Larsen MR. 2012. Characterization of membrane-shed microvesicles from cytokine-stimulated β-cells using proteomics strategies. Molecular & cellular proteomics **11**(8): 230-243.

Parolini I, Federici C, Raggi C, Lugini L, Palleschi S, De Milito A, Coscia C, Iessi E, Logozzi M, Molinari A, Colone M, Tatti M, Sargiacomo M, Fais S. 2009. Microenvironmental pH is a key factor for exosome traffic in tumor cells. Journal of Biological Chemistry **284**(49): 34211-34222.

Pendergrast PS, Pendergrast RS, Pendergrast JS, Markowska AI. 2020. Methods for the isolation of extracellular vesicles and other bioparticles from urine and other biofluids. Washington, DC: U.S. Patent and Trademark Office. U.S. Patent No. 10,669,535.

Perez-Hernandez D, Gutierrez-Vazquez C, Jorge I, Lopez-Martin S, Ursa A, Sánchez-Madrid F, Vázquez J, Yanez-Mo, M. 2013. The intracellular interactome of tetraspanin-enriched microdomains reveals their function as sorting machineries toward exosomes. Journal of Biological Chemistry **288**(17):11649-11661.

Piccin A, Murphy WG, Smith OP. 2007. Circulating microparticles: pathophysiology and clinical implications. Blood reviews **21**(3): 157-171.

Pols MS, Klumperman J. 2009. Trafficking and function of the tetraspanin CD63. Experimental cell research **315**(9): 1584-1592.

Rejraji H, Vernet P, Drevet JR. 2002. GPX5 is present in the mouse caput and cauda epididymidis lumen at three different locations. Molecular Reproduction and Development: Incorporating Gamete Research **63**(1): 96-103.

Reppert N, Lang T. 2022. A conserved sequence in the small intracellular loop of tetraspanins forms an M-shaped inter-helix turn. Scientific Reports **12**(1): 4494.

Ridder K, Keller S, Dams M, Rupp AK, Schlaudraff J, Del Turco D, Starmann J, Macas J, Karpova D, Devraj K, Depboylu C, Landfried B, Arnold B, Plate KH, Höglinger G, Sültmann H, Altevogt P, Momma S. 2014. Extracellular vesicle-mediated transfer of genetic information between the hematopoietic system and the brain in response to inflammation. PLoS biology **12**(6): e1001874.

Roca J, Rodriguez-Martinez H, Padilla L, Lucas X, Barranco I. 2022. Extracellular vesicles in seminal fluid and effects on male reproduction. An overview in farm animals and pets. Animal Reproduction Science **246**: 106853.

Ronquist G, Brody I, Gottfries A, Stegmayr B. 1978. An Mg2+ and Ca2+-stimulated adenosine triphosphatase in human prostatic fluid: part I. Andrologia **10**(4): 261-272.

Sabetian S, Shamsir MS, Naser MA. 2014. Functional features and protein network of human sperm-egg interaction. Systems biology in reproductive medicine **60**(6): 329-337.

Santonocito M, Vento M, Guglielmino MR, Battaglia R, Wahlgren J, Ragusa M, Barbagallo D, Borzì P, Rizzari S, Maugeri M, Scollo P, Tatone C, Valadi H, Purrello M, Di Pietro C 2014. Molecular characterization of exosomes and their microRNA cargo in human follicular fluid: bioinformatic analysis reveals that exosomal microRNAs control pathways involved in follicular maturation. Fertility and sterility **102**(6): 1751-1761.

Schröder J, Lüllmann-Rauch R, Himmerkus N, Pleines I, Nieswandt B, Orinska Z, Koch-Nolte F, Schröder B, Bleich M, Saftig P. 2009. Deficiency of the tetraspanin CD63

associated with kidney pathology but normal lysosomal function. Molecular and cellular biology **29**(4): 1083-1094.

Sohel MMH, Hoelker M, Noferesti SS, Salilew-Wondim D, Tholen E, Looft C, Rings F, Uddin MJ, Spencer TE, Schellander K, Tesfaye D. 2013. Exosomal and non-exosomal transport of extra-cellular microRNAs in follicular fluid: implications for bovine oocyte developmental competence. PloS one **8**(11): e78505.

Stuffers S, Sem Wegner C, Stenmark H, Brech A. 2009. Multivesicular endosome biogenesis in the absence of ESCRTs. Traffic **10**(7): 925-937.

Subedi P, Schneider M, Philipp J, Azimzadeh O, Metzger F, Moertl S, Atkinson MJ, Tapio S. 2019. Comparison of methods to isolate proteins from extracellular vesicles for mass spectrometry-based proteomic analyses. Analytical biochemistry **584**: 113390.

Sullivan R, Saez F. 2013. Epididymosomes, prostasomes, and liposomes: their roles in mammalian male reproductive physiology. Reproduction **146**(1): R21-R35.

Takahashi Y, Bigler D, Ito Y, White JM. 2001. Sequence-specific interaction between the disintegrin domain of mouse ADAM 3 and murine eggs: role of β1 integrin-associated proteins CD9, CD81, and CD98. Molecular biology of the cell **12**(4): 809-820.

Tanigawa M, Miyamoto K, Kobayashi S, Sato M, Akutsu H, Okabe M, Mekada E, Sakakibara K, Miyado M, Umezawa A, Miyado K. 2008. Possible involvement of CD81 in acrosome reaction of sperm in mice. Molecular Reproduction and Development: Incorporating Gamete Research **75**(1): 150-155.

Termini CM, Gillette JM. 2017. Tetraspanins function as regulators of cellular signaling. Frontiers in cell and developmental biology **5**: 34.

Thakur BK, Zhang H, Becker A, Matei I, Huang Y, Costa-Silva B, Zheng Y, Hoshino A, Brazier H, Xiang J, Williams C, Rodriguez-Barrueco R, Silva JM, Zhang W, Hearn S, Elemento O, Paknejad N, Manova-Todorova K, Welte K, Bromberg J, Peinado H, Lyden D. 2014. Double-stranded DNA in exosomes: a novel biomarker in cancer detection. Cell research **24**(6): 766-769.

Théry C, Boussac M, Véron P, Ricciardi-Castagnoli P, Raposo G, Garin J, Amigorena S. 2001. Proteomic analysis of dendritic cell-derived exosomes: a secreted subcellular compartment distinct from apoptotic vesicles. The Journal of Immunology **166**(12): 7309-7318.

Thimon V, Frenette G, Saez F, Thabet M, Sullivan R. 2008. Protein composition of human epididymosomes collected during surgical vasectomy reversal: a proteomic and genomic approach. Human reproduction **23**(8): 1698-1707.

Trajkovic K, Hsu C, Chiantia S, Rajendran L, Wenzel D, Wieland F, Schwille P, Brügger B, Simons M. 2008. Ceramide triggers budding of exosome vesicles into multivesicular endosomes. Science **319**(5867): 1244-1247.

Twenter H, Klohonatz K, Davis K, Bass L, Coleman SJ, Bouma GJ, Bruemmer JE. 2020. Transfer of microRNAs from epididymal epithelium to equine spermatozoa. Journal of equine veterinary science **87**: 102841.

Valadi H, Ekström K, Bossios A, Sjöstrand M, Lee JJ, Lötval JO. 2007. Exosome-mediated transfer of mRNAs and microRNAs is a novel mechanism of genetic exchange between cells. Nature cell biology **9**(6): 654-659.

Van der Pol E, Böing AN, Harrison P, Sturk A, Nieuwland R. 2012. Classification, functions, and clinical relevance of extracellular vesicles. Pharmacological reviews **64**(3): 676-705.

Van Deventer SJ, Dunlock VME, Van Spriel AB. 2017. Molecular interactions shaping the tetraspanin web. Biochemical Society Transactions **45**(3): 741-750.

Van Niel G, Charrin S, Simoes S, Romao M, Rochin L, Saftig P, Marks MS, Rubinstein E, Raposo, G. (2011). The tetraspanin CD63 regulates ESCRT-independent and-dependent endosomal sorting during melanogenesis. Developmental cell **21**(4): 708-721.

van Tilburg M, Sousa S, Lobo MD, Monteiro-Azevedo ACO, Azevedo RA, Araújo AA, Moura AA. 2021. Mapping the major proteome of reproductive fluids and sperm membranes of rams: from the cauda epididymis to ejaculation. Theriogenology **159**: 98-107.

Vyas P, Balakier H, Librach CL. 2019. Ultrastructural identification of CD9 positive extracellular vesicles released from human embryos and transported through the zona pellucida. Systems biology in reproductive medicine **65**(4): 273-280.

Waqas MY, Zhang Q, Ahmed N, Yang P, Xing G, Akhtar M, Basit A, Liu T, Hong C, Arshad M, Rahman HMSU, Chen Q. 2017. Cellular Evidence of Exosomes in the Reproductive Tract of Chinese Soft-Shelled Turtle Pelodiscus sinensis. Journal of Experimental Zoology Part A: Ecological and Integrative Physiology **327**(1): 18-27.

Wolf JP, Monier-Gavelle F, Rubinstein E, Barraud V, Bomsel M, Boucheix C. 2003. Fusion of human gametes requires a CD9 dependent clustering of a6b1 integrin-CD151 complexes on the oocyte membrane. Fertility and Sterility **80**: 80.

Wolf P. 1967. The nature and significance of platelet products in human plasma. British journal of haematology **13**(3): 269-288.

Wubbolts R, Leckie RS, Veenhuizen PT, Schwarzmann G, Möbius W, Hoernschemeyer J, Slot J-W, Geuze HJ, Stoorvogel W. 2003. Proteomic and biochemical analyses of human B cell-derived exosomes: potential implications for their function and multivesicular body formation. Journal of Biological Chemistry **278**(13): 10963-10972.

Xu Z, Xie Y, Zhou C, Hu Q, Gu T, Yang J, Zheng E, Huang S, Xu Z, Cai G, Liu D, Wu Z, Hong L. 2020. Expression pattern of seminal plasma extracellular vesicle small RNAs in boar semen. Frontiers in veterinary science **7**: 585276.

Yanagimachi R, Kamiguchi Y, Mikamo K, Suzuki F, Yanagimachi H. 1985. Maturation of spermatozoa in the epididymis of the Chinese hamster. American Journal of Anatomy **172**(4): 317-330.

Yáñez-Mó M, Barreiro O, Gordon-Alonso M, Sala-Valdés M, Sánchez-Madrid F. 2009. Tetraspanin-enriched microdomains: a functional unit in cell plasma membranes. Trends in cell biology **19**(9): 434-446.

Yáñez-Mó M, Siljander PRM, Andreu Z, Zavec AB, Borràs FE, Buzas EI, Buzas K, Casal E, Cappello F, Carvalho J, Colás E, Cordeiro-da Silva A, Fais S, Falcon-Perez JM, Ghobrial IM, Giebel B, Gimona M, Graner M, Gursel I, Gursel M, Heegaard NHH, Hendrix A, Kierulf P, Kokubun K, Kosanovic M, Kralj-Iglic V, Krämer-Albers EV, Laitinen S, Lässer C, Lener T, Ligeti E, Linē A, Lipps G, Llorente A, Lötvall J, Manček-Keber M, Marcilla A, Mittelbrunn M, Nazarenko I, Nolte-‘t Hoen ENM, Nyman TA, O'Driscoll L, Olivan M, Oliveira C, Pállinger E, del Portillo HA,Reventós J, Rigau M, Rohde E, Sammar

M, Sánchez-Madrid F, Santarém N, Schallmoser K, Ostenfeld MS, Stoorvogel W, Stukelj R, Van der Grein SG, Vasconcelos MH, Wauben MHM, De Wever O. 2015. Biological properties of extracellular vesicles and their physiological functions. Journal of Extracellular Vesicles **4**(1): 2001-3078.

Yang Y, Liu XR, Greenberg ZJ. 2020. Open conformation of tetraspanins shapes interaction partner networks on cell membranes. The EMBO Journal **39**(18): e105246.

Yue B, Yang H, Wang J, Ru W, Wu J, Huang Y, Lan X, Lei C, Chen H. 2020. Exosome biogenesis, secretion and function of exosomal miRNAs in skeletal muscle myogenesis. Cell proliferation **53**(7): e12857.

Zaborowski MP, Balaj L, Breakefield XO, Lai CP. 2015. Extracellular vesicles: composition, biological relevance, and methods of study. Bioscience **65**(8): 783-797.

Zarovni N, Corrado A, Guazzi P, Zocco D, Lari E, Radano G, Muhhina J, Fondelli C, Gavrilova J, Chiesi A. 2015. Integrated isolation and quantitative analysis of exosome shuttled proteins and nucleic acids using immunocapture approaches. Methods **87**: 46-58.

Zhang M, Jin K, Gao L, Zhang Z, Li F, Zhou F, Zhang L. 2018. Methods and technologies for exosome isolation and characterization. Small Methods **2**(9): 1800021.

Zhang Y, Bi J, Huang J, Tang Y, Du S, Li P. 2020. Exosome: a review of its classification, isolation techniques, storage, diagnostic and targeted therapy applications. International journal of nanomedicine: 6917-6934.

Zhang Y, Liu Y, Liu H, Tang WH. 2019. Exosomes: biogenesis, biologic function and clinical potential. Cell & bioscience **9**(1): 1-18.

Zhang Z, Wang C, Li T, Liu Z, Li L. 2014. Comparison of ultracentrifugation and density gradient separation methods for isolating Tca8113 human tongue cancer cell line-derived exosomes. Oncology letters **8**(4): 1701-1706.

Zhou GB, Liu GS, Meng QG. 2009. Tetraspanin CD9 in bovine oocytes and its role in fertilization. Journal of Reproduction and Development **55**(3): 305-308.

Zhou M, Weber SR, Zhao Y, Chen H, Sundstrom JM. 2020. Methods for exosome isolation and characterization. Exosomes: 23-38.

Zimmerman B, Kelly B, McMillan BJ, Seegar TC, Dror RO, Kruse AC, Blacklow SC. 2016. Crystal structure of a full-length human tetraspanin reveals a cholesterol-binding pocket. Cell **167**(4): 1041-1051.

Ziyyat A, Rubinstein E, Monier-Gavelle F, Barraud V, Kulski O, Prenant M, Boucheix C, Bomsel M, Wolf JP. 2006. CD9 controls the formation of clusters that contain tetraspanins and the integrin α6β1, which are involved in human and mouse gamete fusion. Journal of cell science **119**(3): 416-424.

Zou F, Wang X, Han X, Rothschild G, Zheng SG, Basu U, Sun J. 2018. Expression and function of tetraspanins and their interacting partners in B cells. Frontiers in immunology **9**: 1606.

8 Appendix

8.1 Tables

Table 1: Exosomal protein content identified by MS (acidic conditions).

Acidic conditions						
Name	Avg. Mass	No of Peptides	No of Unique Peptides	Coverage (%)	Intensity	-10lgP
Carbohydrate-binding protein AQN-3	12885	12	6	81	2.40E+04	466.83
Major seminal plasma glycoprotein PSP-II	14816	14	14	65	4.64E+04	445.86
Seminal plasma sperm motility inhibitor	15203	9	3	51	5.91E+03	412.69
Major seminal plasma glycoprotein PSP-I	14501	10	10	65	1.52E+04	412.37
Carbohydrate-binding protein AWN	16730	10	10	50	2.63E+04	401.7
Carbohydrate-binding protein AQN-1	11882	8	8	93	7.96E+03	369.35
Trypsin	24409	5	5	34	2.58E+04	342.02
Albumin	69692	8	8	17	1.39E+03	297.75
Seminal plasma protein pB1	15373	5	5	28	9.74E+03	278.93
Lactotransferrin	77626	5	5	9	2.04E+03	266.98
Actin cytoplasmic 1	41737	5	5	19	3.71E+03	263.33
Sperm-associated acrosin inhibitor	11141	4	4	41	3.75E+03	220.44
Clusterin	51775	5	5	12	1.01E+03	218.96
Hemoglobin subunit alpha	15039	2	2	18	2.02E+03	205.52
NPC intracellular cholesterol transporter 2	16288	3	3	46	5.98E+02	187.39
Hemoglobin subunit beta	16166	3	3	28	6.37E+02	178.34
Aminopeptidase N	108832	1	1	1	3.64E+02	141.35
Deleted in malignant brain tumors 1 protein	132225	2	2	2	9.91E+02	139.14
Tubulin beta chain	49861	4	4	12	1.90E+02	120.87
Myosin light polypeptide 6	16930	2	2	16	1.92E+02	107.88
Annexin A2	38542	1	1	3	1.55E+03	103.99
CD59 glycoprotein	13790	1	1	9	2.00E+02	103.93
Glutathione hydrolase 1 proenzyme	61316	2	2	3	2.21E+02	99.56
Heat shock protein beta-1	22942	1	1	8	1.95E+02	97.02
Inter-alpha-trypsin inhibitor heavy chain H4	102146	1	1	1	0.00E+00	94.69
Tubulin alpha-1A chain	50069	1	1	3	0.00E+00	93.62
C-type natriuretic peptide	13243	1	1	7	1.45E+02	92.96
Ig lambda chain C region	11003	1	1	16	1.78E+02	87.85
Lactadherin	45725	1	1	3	0.00E+00	86.05
Beta-hexosaminidase subunit beta	61050	1	1	2	9.65E+02	84.15
Ubiquitin-60S ribosomal protein L40	14728	1	1	10	0.00E+00	77
Polyubiquitin-C	59993	1	1	2	0.00E+00	77
Moesin	67661	1	1	2	0.00E+00	66.99
Radixin	68550	1	1	2	0.00E+00	66.99
Pro-cathepsin H	37455	1	1	4	0.00E+00	66.42
Growth hormone receptor	71145	1	1	2	7.12E+02	63.56
Inhibitor of carbonic anhydrase	77634	1	1	1	2.16E+02	62.65
Heat shock protein HSP 90-alpha	84775	1	1	1	0.00E+00	50.13
Oviduct-specific glycoprotein	58519	1	1	2	0.00E+00	46.77
Heat shock 70 kDa protein (Fragment)	42290	1	1	2	3.01E+02	40.66
Heat shock 70 kDa protein 6	71109	1	1	1	3.01E+02	40.66
Glutamyl aminopeptidase	108284	0	0	0		37.88

Cytoskeletal protein
Protease
Transfer/carrier protein
Chaperone
Protease inhibitor
Transmemb. signal receptor
Spermadhezins
Unmapped protein

Table 2: Exosomal protein content identified by MS (basic conditions).

Basic conditions						
Name	**Avg. Mass**	**No of Peptides**	**No of Unique Peptides**	**Coverage (%)**	**Intensity**	**-10lgP**
Major seminal plasma glycoprotein PSP-I	14501	8	8	62	2.85E+04	398.08
Major seminal plasma glycoprotein PSP-II	14816	8	8	57	2.55E+04	395.18
Carbohydrate-binding protein AWN	16730	7	7	39	2.47E+04	383.15
Carbohydrate-binding protein AQN-3	12885	8	4	76	1.78E+04	380.22
Trypsin	24409	6	6	40	1.58E+04	367.7
Actin cytoplasmic 1	41737	9	3	27	2.47E+03	348.65
Actin alpha skeletal muscle	42051	7	1	20	2.51E+03	325.77
Seminal plasma sperm motility inhibitor	15203	5	1	49	6.71E+03	321
Carbohydrate-binding protein AQN-1	11882	5	5	73	4.85E+03	319.96
Seminal plasma protein pB1	15373	5	5	22	9.78E+03	281.66
Sperm-associated acrosin inhibitor	11141	7	7	54	1.63E+04	280.61
Albumin	69692	6	6	12	1.22E+03	272.25
Clusterin	51775	8	8	17	3.41E+03	263.44
Lactotransferrin	77626	2	2	4	6.85E+02	203.34
Glutathione hydrolase 1 proenzyme	61316	3	3	7	1.20E+03	192.96
NPC intracellular cholesterol transporter 2	16288	4	4	30	6.80E+02	184.24
C-type natriuretic peptide	13243	3	3	21	3.34E+02	171.32
Beta-microseminoprotein	12246	3	3	31	3.37E+03	165.04
Thymosin beta-4	5053	2	2	32	3.44E+02	162.16
Beta-hexosaminidase subunit beta	61050	2	2	4	2.80E+02	140.34
Radixin	68550	2	2	3	3.74E+02	140.12
Inter-alpha-trypsin inhibitor heavy chain H4	102146	1	1	1	0.00E+00	108.43
Ubiquitin-60S ribosomal protein L40	14728	1	1	10	5.06E+02	107.73
Polyubiquitin-C	59993	1	1	2	5.06E+02	107.73
Aminopeptidase N	108832	1	1	1	0.00E+00	78.67
Chloride intracellular channel protein 1 (Fragmen	12184	1	1	8	2.76E+02	76.65
Spike glycoprotein	149493	1	1	1	0.00E+00	57.98
Spike glycoprotein	149648	1	1	1	0.00E+00	57.98
Tropomyosin alpha-1 chain	32707	1	1	4	5.85E+02	50.27
Tropomyosin alpha-3 chain	33058	1	1	4	5.85E+02	50.27
Probable nuclear antigen	172166	1	1	1	0.00E+00	47.39
Membrane protein	29587	1	1	5	0.00E+00	46.6
Membrane protein	29611	1	1	5	0.00E+00	46.6
Uncharacterized protein DP238L	28208	1	1	4	2.25E+02	43.13
Beta-2-microglobulin	13362	1	1	10	2.30E+02	42.61

8.2 Abbreviations

AA amino acid

ALIX programmed cell death 6-interacting protein

ApoBDs apoptotic bodies

AR acrosome reaction

CD cluster differentiation

Cer ceramide

circRNA circular RNA

DGUC density gradient ultracentrifugation

DNase deoxyribonuclease

dsDNA double-stranded DNA

dUC differential ultracentrifugation

ELISA enzyme-linked immunosorbent assay

ESCRT endosomal sorting complexes required for transport

EVs extracellular vesicles

FF follicular fluid

HSP heat shock protein

IA immunoaffinity capture-based techniques

ILVs intraluminal vesicles

LAMP lysosomal-associated membrane proteins

LEL large extracellular loop

lncRNA long non-coding RNA

miRNA microRNA

mRNA messenger RNA

MS mass spectrometry

mtDNA / mtRNA mitochondrial DNA/RNA

MVBs multivesicular bodies

MVs microvesicles

nSMase neutral sphingomyelinase

OF oviductal fluid

OVs oviductosomes

PA phosphatidic acid

PBS phosphate-buffered saline

piRNA piwi-interacting RNA

PLD phospholipase D

PMCA4 plasma membrane calcium ATPase

PTMs post-translational modifications

PVS perivitelline space

RBP RNA-binding protein

RNase ribonuclease

RNP ribonucleoprotein particle

rRNA ribosomal RNA

RT room temperature

SEL small extracellular loop

SM sphingomyelin

snoRNA small nucleolar RNA

snRNA small nuclear RNA

SP seminal plasma

ssDNA single-stranded DNA

TCA trichloroacetic acid

TEM transmission electron microscopy

TM transmembrane microdomains

TNBC triple-negative breast cancer

tRNA transfer RNA

Tsg101 tumor susceptibility gene 101

UF ultrafiltration

VPS4 vacuolar protein sorting-associated protein 4A

ZP zona pellucida